4-22-2019

Aedes aegypti Mosquitoes Detect Acidic Volatiles Found in Human Odor Using the IR8a Pathway

Joshua A. Raji

John S. Casti

Sheyla Gonzalez

Valeria Saldana

Marcus C. Stensmyr

See next page for additional authors

Authors

Joshua A. Raji, John S. Casti, Sheyla Gonzalez, Valeria Saldana, Marcus C. Stensmyr, and Matthew DeGennaro

Article

Current Biology

Aedes aegypti Mosquitoes Detect Acidic Volatiles Found in Human Odor Using the IR8a Pathway

Graphical Abstract

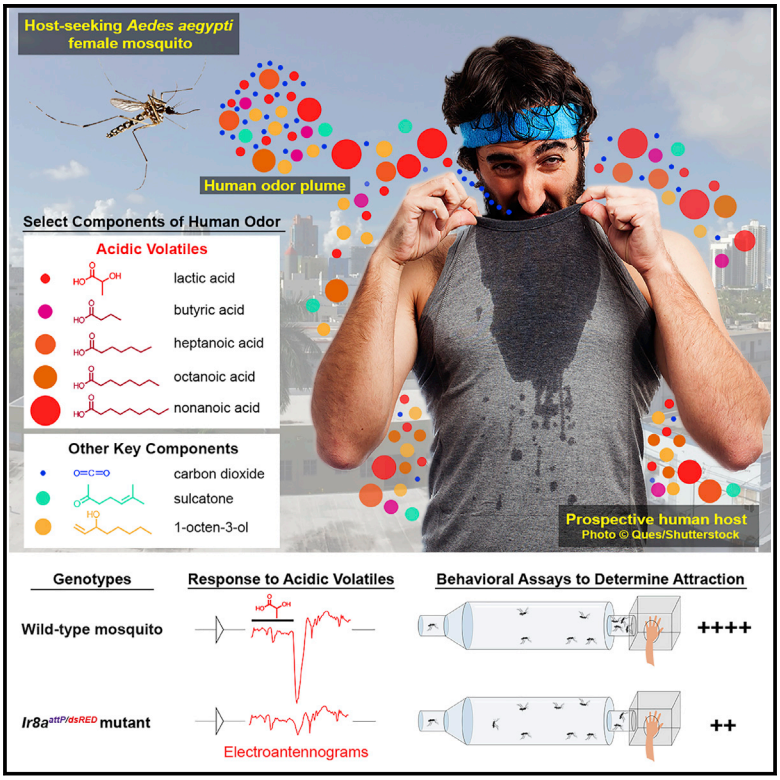

Highlights

- *Ae. aegypti Ir8a* mutant mosquitoes cannot sense lactic acid, a human sweat component
- Attraction to humans and human odor is reduced in *Ir8a* mutant mosquitoes
- *Ae. aegypti* IR8a pathway responds to human-odor cues during blood feeding
- The *Ir8a* mutant host-seeking defect cannot be rescued by other olfactory receptors

Authors

Joshua I. Raji, Nadia Melo, John S. Castillo, Sheyla Gonzalez, Valeria Saldana, Marcus C. Stensmyr, Matthew DeGennaro

Correspondence

mdegenna@fiu.edu

In Brief

Raji et al. show that *Ae. aegypti* mosquitoes use the olfactory coreceptor, IR8a, to detect humans and human odor. IR8a responds to acidic volatiles found in human odor, including lactic acid, a component of human sweat. This study highlights the crucial role acidic volatiles play when mosquitoes target a host for blood feeding.

Raji et al., 2019, Current Biology *29*, 1253–1262
April 22, 2019
https://doi.org/10.1016/j.cub.2019.02.045

CellPress

Current Biology
Article

CellPress

Aedes aegypti Mosquitoes Detect Acidic Volatiles Found in Human Odor Using the IR8a Pathway

Joshua I. Raji,[1] Nadia Melo,[2] John S. Castillo,[1] Sheyla Gonzalez,[1] Valeria Saldana,[1] Marcus C. Stensmyr,[2] and Matthew DeGennaro[1,3,*]
[1]Department of Biological Sciences & Biomolecular Sciences Institute, Florida International University, Miami, FL 33199, USA
[2]Department of Biology, Lund University, 22362 Lund, Sweden
[3]Lead Contact
*Correspondence: mdegenna@fiu.edu
https://doi.org/10.1016/j.cub.2019.02.045

SUMMARY

Mosquitoes use olfaction as a primary means of detecting their hosts. Previously, the functional ablation of a family of *Aedes aegypti* olfactory receptors, the odorant receptors (ORs), was not sufficient to reduce host seeking in the presence of carbon dioxide (CO_2). This suggests the olfactory receptors that remain, such as the ionotropic receptors (IRs), could play a significant role in host detection. To test this, we disrupted the *Ir8a* co-receptor in *Ae. aegypti* using CRISPR/Cas9. We found that *Ir8a* mutant female mosquitoes are not attracted to lactic acid, a behaviorally active component of human sweat, and they lack odor-evoked responses to acidic volatiles. The loss of *Ir8a* reduces mosquito attraction to humans and their odor. We show that the CO_2-detection pathway is necessary but not sufficient for IR8a to detect human odor. Our study reveals that the IR8a pathway is crucial for an anthropophilic vector mosquito to effectively seek hosts.

INTRODUCTION

Anthropophilic female mosquitoes, such as *Aedes aegypti* and *Anopheles gambiae*, have a strong innate drive to find their human hosts and obtain blood meals, which are required for their egg production. As has been highlighted by the recent Zika outbreak, *Aedes* mosquitoes are efficient vectors for pathogen transmission because of their host-seeking behavior and susceptibility for infection by flaviviruses [1]. Female mosquitoes, like other hematophagous Diptera, integrate an array of sensory information to find their human hosts, including carbon dioxide (CO_2), body odor, heat, moisture, and visual cues [2]. How these different cues are sensed to enable mosquito host-seeking has only begun to be understood. Among these attractive cues, human body odor is a complex blend of volatile chemicals that distinguishes us from other vertebrate hosts [3]. Skin microbiota plays a large role in generating the volatile compounds that attract mosquitoes to human sweat [4]. In *Ae. aegypti* and *An. gambiae*, human odors that elicit both electrophysiological and behavioral responses have been identified including ammonia, amines, carboxylic acids, lactic acid, ketones, sulfides, and 1-octen-3-ol [5–10].

Insects respond to volatile chemicals in the environment with a complex repertoire of olfactory receptors that are evolutionarily distinct from vertebrate olfactory receptors [11]. Two families of odor-gated ion channels that respond to a diverse set of molecules, the odorant receptors (ORs) and the ionotropic receptors (IRs) [12–14], have been identified in insects. In addition, there are also gustatory receptors (GRs) that are highly sensitive to CO_2 [15–17]. Odor-tuned ORs rely upon the obligate olfactory co-receptor Orco to form an odor-gated ion channel complex [18–20]. In *Ae. aegypti*, loss of *orco* results in a loss of electrophysiological responses to some but not all odorants [21]. In the presence of CO_2, attraction to human odor was not significantly different from wild-type controls in female *Ae. aegypti orco* mutants. However, in the absence of CO_2, *orco* mutants lose strong attraction to human odor. *Ae. aegypti* mutants lacking *Gr3*, a subunit of the heteromeric CO_2 receptor complex, show no electrophysiological or behavioral responses to CO_2 [22]. Behavioral analysis of *Gr3* mutants showed that CO_2 can gate multiple cues that are sensed by mosquitoes, including heat and human odor.

Drosophila IRs are expressed in olfactory sensory neurons (OSNs) that are distinct from OR and GR lineages [23]. There are at least two IR co-receptors, IR8a and IR25a, and a putative third, IR76b [14, 24]. These co-receptors form an odor-responsive ion channel with other odor-tuned IRs. For example, some *Drosophila* odor-tuned IRs require IR8a as a co-receptor, while some other odor-tuned IRs form a functional complex with IR25a and/or IR76b, but not with all three co-receptors. Similarly, some OSNs have been shown to express both IR8a and IR25a protein [24]. There are 30 putative odor-tuned IRs expressed in the *Ae. aegypti* antennae that could potentially form an odor-responsive ion channel with any of the IR co-receptors [25]. The combinatorial pattern of expression observed in IRs may allow flexibility in responding to more diverse olfactory cues with fewer odor-tuned receptors than the Orco pathway [24], which encompasses at least 117 odor-tuned ORs [26].

Insect IRs have been reported to detect amines, aldehydes, ketones, and acids [10, 14, 23, 27, 28]. Since many of these compounds are not represented in the OR chemical space, which includes alcohols and esters, the IR odor ligands are largely complementary and do not overlap with OR odor ligands [23, 29]. In *Drosophila*, *Ir25a* and *Ir76b* are necessary for odor-evoked electrophysiological responses to amines [30], whereas receptor

neurons expressing *Ir8a* are tuned to volatile acids [24]. IR8a forms a functional complex with AgIR75k to elicit odor-evoked inward currents in response to carboxylic acids including heptanoic acid, octanoic acid, and nonanoic acid [10]. Lactic acid is more enriched in human skin emanations than in those of other vertebrates and may be one of the cues that signals to the mosquito that the target host is a human [31]. How lactic acid is sensed in mosquitoes is unknown, but it is likely to be IR dependent.

Whereas *Drosophila Ir25a* is involved in many functions, including olfaction, taste, hygrosensation, thermosensation, and attraction to CO_2 [24, 30, 32–40], *Ir8a* appears to function exclusively in detecting odors and is not necessary for attractive responses to CO_2 [24, 27, 28, 40]. In *Ae. aegypti*, *Ir8a* expression is localized to the antennae and cannot be detected in other chemosensory tissues, whereas *Ir25a* is broadly expressed in multiple chemosensory tissues and is three times more abundant in sugar-fed female mosquito antennae than is *Ir8a* [25]. Similarly, *Ir8a* transcript abundance was detected only in the antennae of *An. gambiae* adults [41, 42]. These results make *Ir8a* a likely candidate receptor for odor detection during mosquito host-seeking behavior. *Ir25a* and *Ir76b* have broader expression patterns that are consistent with these receptors being involved in other sensory modalities in addition to olfaction [24, 25, 30, 32].

Since host seeking is not completely ablated in *orco* or *Gr3* mutants [21, 22], we reasoned that the IR olfactory receptors retained in these mutants are crucial for host-seeking. Here, we used the CRISPR/Cas9 system to disrupt *Ae. aegypti Ir8a.* We tested the relative contribution of *Ir8a* in human-odor detection and its genetic interaction with other olfactory receptor pathways that have been previously implicated in *Ae. aegypti* host seeking. We found that *Ir8a* mutants are not attracted to lactic acid, a behaviorally active component of human sweat, nor were they able to detect acidic components of human odor. When compared to wild-type controls in membrane blood-feeding assays, *Ir8a* mutants have reduced responses to human odor but not to heat and CO_2. *Ir8a* mutants are also less responsive to humans and human odor than wild-type controls in uniport olfactometer assays. The genetic interactions of *Ir8a* and *orco* as well as *Ir8a* and *Gr3* suggest a crucial role for CO_2 in sensitizing mosquitoes to human odor and highlights the importance of human acidic volatile detection during mosquito host seeking.

RESULTS

Targeted Mutagenesis of *Ae. aegypti Ir8a*, an Antenna-Specific Ionotropic Receptor

Previous analysis of the neurotranscriptome of *Ae. aegypti* has suggested that *Ir8a* is expressed in the antennae and no other chemosensory tissues [25]. To confirm this result, we first asked if *Ir8a* expression can be detected in any other body tissues. Using quantitative RT-PCR analysis in wild-type mosquitoes, we compared the expression of the intact female to that of the head plus antennae, antennae, body minus the head, and head minus antennae. We show that *Ir8a* mRNA expression is enriched in the antennae and nearly undetectable in other tissues (Figure S1A). Given that olfaction is key for mosquitoes to host seek [2] and *Ir8a* acts as an obligate olfactory co-receptor that can complex with odor-tuned IRs that detect acids in *Drosophila* [24, 28], we speculated that mutations in *Ae. aegypti Ir8a* should disrupt a distinct subset of IRs that are responsive to acidic volatiles in human odor.

To test this hypothesis, we generated targeted null mutations in the *Ae. aegypti Ir8a* gene using CRISPR/Cas9 RNA-guided gene editing [43]. We integrated two distinct donor DNAs to generate two independent alleles in the *Ir8a* locus at exon 2 and exon 3 (see STAR Methods). These two independent mutant alleles, $Ir8a^{dsRED}$ (exon 2) and $Ir8a^{attP}$ (exon 3), are predicted to produce truncated IR8a proteins that would eliminate *Ir8a* function. The sgRNA was designed to guide the Cas9 endonuclease to exon 2 of *Ir8a* and enable integration of the polyubiquitin promoter and dsRED fluorescent protein through homology-dependent repair by way of a plasmid containing the promoter, fluorescent marker, and SV40 terminator flanked by homologous DNA sequences surrounding the predicted cut site (Figure 1A). This insertion visually marked $Ir8a^{dsRED}$ mutants with dsRED fluorescence and could be detected in the *Ir8a* locus by PCR using a primer that anneals to sequences in the donor construct homologous right arm in *Ir8a* exon 2 and a second primer that anneals outside the bounds of the donor construct in *Ir8a* exon 4 (Figures 1B and 1C; Table S1). Sanger sequencing of this PCR amplicon showed site-directed integration of the donor plasmid into the *Ir8a* locus as expected (Data S1; Table S1). To generate the $Ir8a^{attP}$ allele, an sgRNA, Cas9 mRNA, and a single-stranded DNA oligo containing a 50 bp *attP* PhiC31 recombination site flanked by 75 bp of homologous sequence surrounding the CRISPR binding site were injected into preblastoderm embryos. However, we observed a 17 bp deletion in the CRISPR site and 2 bp deletion in the *attP* site, which may reduce PhiC31-mediated recombination frequency at this site. $Ir8a^{attP}$ sequencing data suggests that it was a null mutation, as the predicted mRNA from the $Ir8a^{attP}$ allele would contain 20 stop codons (Data S2). To reduce the possibility of off-target effects, both alleles were outcrossed to the wild-type Orlando laboratory strain for five generations and then homozygosed.

We next investigated if *Ir8a* mRNA is disrupted in *Ir8a* mutants. Using quantitative RT-PCR, *Ir8a* mRNA in the homozygous $Ir8a^{attP/attP}$ mutants was nearly undetectable in both sexes (Figures S1B and S1C). This suggests that the mRNA is degraded by non-sense-mediated decay and that the $Ir8a^{attP/attP}$ mutant is an RNA null. However, the $Ir8a^{dsRED}$ allele showed overexpression of *Ir8a* mRNA in male and female mutants (Figures S1B and S1C). The increase in *Ir8a* transcript levels observed in the $Ir8a^{dsRED}$ allele is likely the result of the insertion of the polyubiquitin promoter dsRed fluorescent protein expression cassette into the locus. The predicted $Ir8a^{dsRED}$ transcript cannot produce a full-length IR8a protein (Data S1). No behavioral phenotypic differences were found between the mosquitoes carrying these alleles, suggesting that both $Ir8a^{attP}$ and the $Ir8a^{dsRED}$ alleles are null (see below).

A concern with the application of CRISPR/Cas9 mutagenesis is off-target mutations, which may alter the function of other genes [44]. To rule out non-specific behavioral defects in the *Ir8a* mutants, we assessed their fitness. Using a locomotor activity assay, we found no difference in activity in *Ir8a* mutants, when compared to the wild-type and heterozygous controls, in the number of times they moved past an infrared beam (Figures

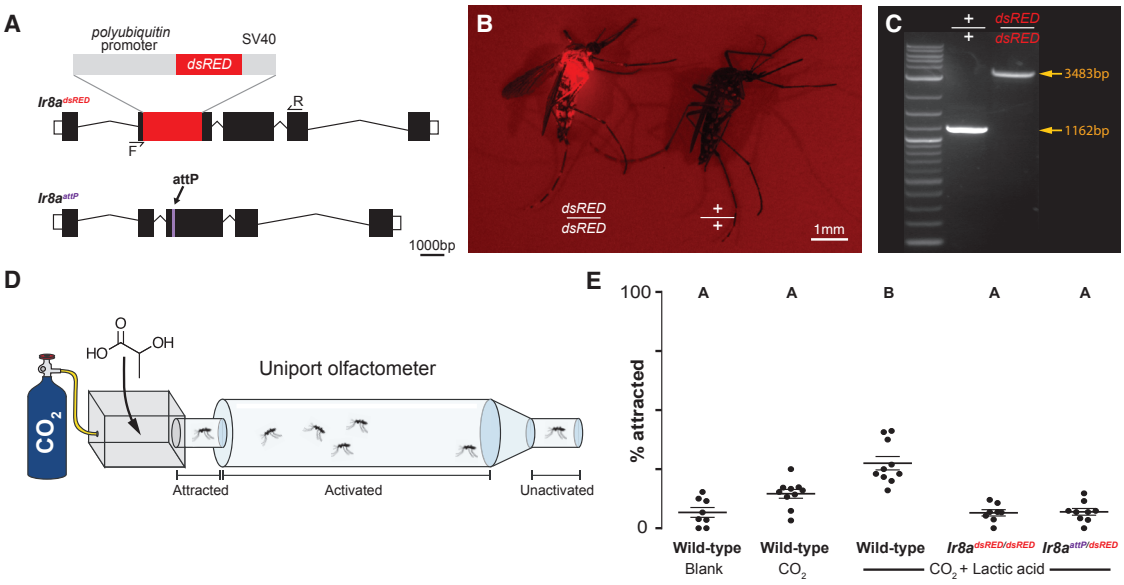

Figure 1. Mutagenesis of the *Ae. aegypti Ir8a* Locus and Behavioral Phenotypic Analysis of *Ir8a* Mutant Response to Lactic Acid

(A) CRISPR sgRNAs designed to target the Cas9 nuclease to exon 2 and exon 3 of *Ir8a*. Integration location of the dsRED fluorescent marker and ssODN containing *attP* site into exon 2 and exon 3 of *Ir8a* are shown, respectively.

(B) dsRED fluorescence in the $Ir8a^{dsRED/dsRED}$ homozygous mutant (left) and wild-type (right) adult female mosquitoes.

(C) PCR amplification from *Ir8a* exon 2 locus; note 1162 bp amplicon from the wild-type *Ir8a* locus versus the larger 3483 bp amplicon from $Ir8a^{dsRED/dsRED}$ homozygous mutant female mosquitoes.

(D) Uniport olfactometer assay designed to test behavioral response of *Ir8a* mutants to lactic acid. Mosquitoes that fail to leave the trap during the assay are scored as unactivated, whereas mosquitoes that leave the trap but remain in the main tunnel are scored as activated. Mosquitoes in the trap adjacent to the stimulus chamber are scored as attracted.

(E) Percent of female mosquitoes attracted to no odor (blank) and CO_2 alone (CO_2) as well as to CO_2 and lactic acid in a uniport olfactometer. Lactic acid and CO_2 were co-presented to wild-type, $Ir8a^{dsRED/dsRED}$, and $Ir8a^{attP/dsRED}$ female mosquitoes (right three panels). The horizontal bar indicates the mean. Error bars show the standard error. Dots represent individual trials. Different letters mark whether a group of trials is significantly different ($p < 0.0001$, $n = 8–10$). Analysis was done using one-way ANOVA with post hoc Tukey's HSD test. See also Figures S1 and S2 Table S1, and Data S1 and S2.

S2A and S2B) [21]. We further investigated if *Ir8a* mutants may have feeding defects using the capillary feeder assay (CAFE) (Figure S2C) [45, 46]. In this assay, mosquitoes were allowed to feed through a calibrated capillary tube containing a 10% sucrose solution. We quantified sucrose consumption by recording the change in volume relative to that in control vials without mosquitoes. We recorded no difference in feeding in *Ir8a* mutants when compared to the wild-type and heterozygous controls after 18 h of *ad libitum* feeding (Figure S2D). We also evaluated the ability of the *Ir8a* mutants to survive fasting. This was tested by sugar starving mosquitoes that had access to water [21]. Our results suggest that our *Ir8a* mutant males and females can resist starvation as well as wild-type and heterozygous controls could. (Figures S2E and S2F). Taken together, these studies attest to the fitness of *Ir8a* mutants as well as their suitability for further behavioral analysis.

The IR8a Pathway Is Required for Sensing and Responding Behaviorally to Acidic Volatiles

Lactic acid has been previously identified to be a behaviorally active component of human sweat, which has been used to lure mosquitoes into traps or attract mosquitoes in olfactometer assays, but olfactory receptors for the compound have not been identified [5, 8, 10, 47]. Lactic acid by itself is not attractive to mosquitoes [5]. However, both lactic acid and CO_2 can synergize when presented together to elicit attraction [22, 31]. Using a uniport olfactometer with carbon-filtered air flow, we tested the responses of wild-type and *Ir8a* mutant female mosquitoes to filtered air and CO_2 as well as to lactic acid and CO_2 (Figures 1D and 1E). In order to control for recessive background mutations that may have occurred in either of the two lines, we tested $Ir8a^{dsRED/dsRED}$ and heteroallelic *Ir8a* mutants ($Ir8a^{attP/dsRED}$). The responses of $Ir8a^{dsRED/dsRED}$ and $Ir8a^{attP/dsRED}$ mutants to lactic acid and CO_2 were not significantly different from each other or from the wild-type responses to CO_2 alone or to filtered air (blank) (Figure 1E).

To confirm that *Ir8a* mutants have lost the ability to detect lactic acid, we examined the electrophysiological responses of female mosquitoes to a panel of odors. Unlike that in *Drosophila*, the olfactory receptor expression pattern in mosquitoes has not been comprehensively mapped [48, 49]. The locations of IR8a-expressing olfactory receptor neurons in the antennae is unknown, making single sensillum recordings difficult to perform. To overcome this limitation, we used electroantennogram (EAG) measurements (Figure 2), which record the average signal output from the entire mosquito antenna for a given odor volatile [50]. The wild-type mosquitoes showed robust odor-evoked responses to all the odor panels tested (Figure 2A). However, $Ir8a^{dsRED/dsRED}$ mutants are insensitive to the acidic components of human odor represented in the panel, including lactic acid

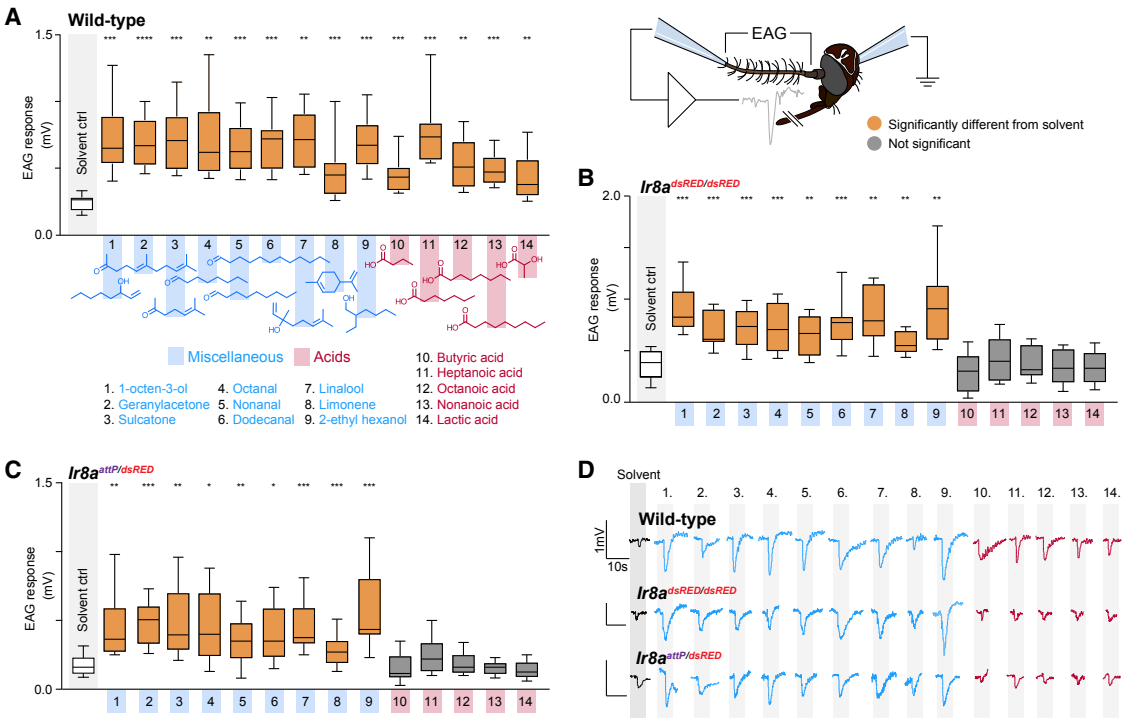

Figure 2. IR8a Olfactory Receptor Pathway Is Required for Sensing Acidic Volatiles That Are Components of Human Odor

(A–C) Electroantennogram (EAG) responses of wild-type Orlando strain (A), *Ir8a*$^{dsRED/dsRED}$ mutants (B), and heteroallelic *Ir8a*$^{dsRED/attP}$ (C) to volatiles that are components of human odor.

(D) Representative EAG traces of the wild-type and *Ir8a* mutant mosquitoes. This figure is represented by a min-max box and whisker plot. The ends of the box are the upper and lower quartiles. The median is marked by a horizontal line inside the box. The whiskers are the two lines outside the box that extend to the highest and lowest EAG response. The odors marked in red are acidic volatiles, while the odors represented in blue include alcohols, ketones, aldehydes, monoterpenoid, and alkene. EAG responses represented in orange dots are significantly different from the solvent control. Responses labeled in gray are not significantly different from the solvent control. Statistical analysis was done using a mixed-effects model with Dunnet's multiple comparison test. Each column was compared with the mean of the solvent control column. EAG responses marked with asterisks indicate that it is significantly different from response to the control solvent (*$p < 0.01$, **$p < 0.001$, ***$p < 0.0001$, and ****$p < 0.00001$).

(Figure 2B). We observed a similar lack of olfactory sensitivity in *Ir8a*$^{attP/dsRED}$ heteroallelic mutants (Figure 2C). As shown on the representative current traces (Figure 2D), *Ir8a*$^{dsRED/dsRED}$ and *Ir8a*$^{attP/dsRED}$ olfactory receptor neurons show weak responses to acidic volatiles, similar to the solvent response of wild-type controls.

Our results show that *Ir8a* mutants have lost their behavioral and electrophysiological responses to lactic acid and strongly suggest that IR8a is required to detect lactic acid. This was true of both the *Ir8a*^{dsRED} allele and the heteroallelic combination of the *Ir8a*^{dsRED} allele and the RNA null *Ir8a*^{attP} allele, suggesting that both alleles retain no *Ir8a* gene function. In our study, *Ir8a* mutants are still able to detect other human volatile compounds including some alcohols, aldehydes, and ketones, suggesting that other olfactory pathways are not impaired in these mutants.

Ae. aegypti IR8a Pathway Responds to Human Odor Cues during Blood Feeding

Using a membrane blood-feeding assay (Figure 3A), we assessed the responses of *Ir8a* mutant and control female mosquitoes to heat, CO_2, and human-odor cues by determining the percentage of females that would blood feed [22]. While CO_2 and human odor can activate and elicit mosquito attraction toward a blood source, the temperature of the meal is crucial for feeding to occur [51]. Experiments carried out with wild-type mosquitoes showed a robust feeding response when all cues were present, but feeding was reduced when human odor, CO_2, or heat was removed (Figure 3B). In the presence of all three cues, we found that both the *Ir8a*$^{dsRED/dsRED}$ and the heteroallelic *Ir8a*$^{attP/dsRED}$ mutants exhibited reduced blood feeding when compared to wild-type or heterozygous controls (Figure 3C).

We attempted to determine the individual contributions of human odor, CO_2, and heat cues in the assay to the *Ir8a* mutant phenotype by eliminating one cue at a time. When only heated blood and CO_2 were used as attractants, there was no significant difference among genotypes (Figure 3D). This suggests that *Ir8a* mutant females can respond similarly to these cues as wild-type females. When the CO_2 source was removed from the assay, the rate of blood feeding was very low across all the genotypes (Figure 3E). Similarly, when the temperature of the blood was shifted from body temperature (37°C) to ambient temperature (26°C), the absence of the heat cue nearly eliminated blood feeding across all genotypes (Figure 3F). The level of blood feeding was very low in the absence of heated blood or CO_2, so it is difficult to discern genotypic differences. By comparing the results

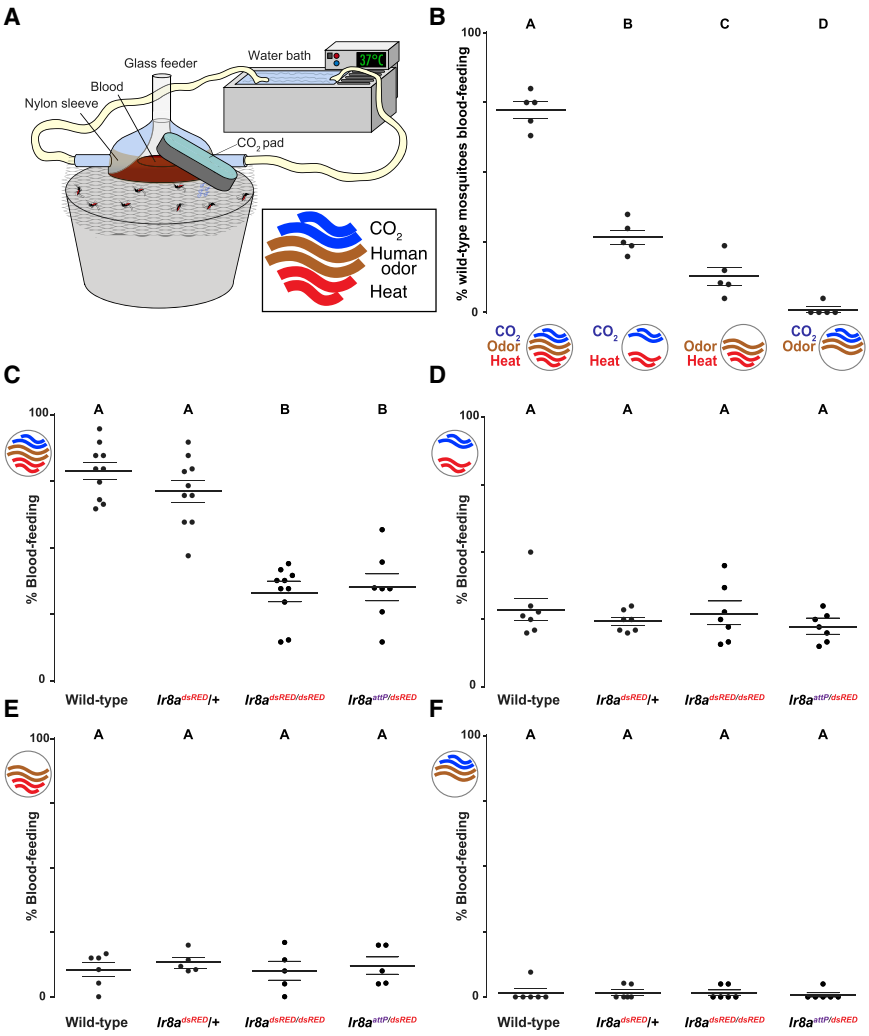

Figure 3. *Ae. aegypti* IR8a Pathway Responds to Human Odor Cues during Blood Feeding

(A) Illustration showing the membrane-feeding assay to simulate female mosquito blood-feeding behavior.

(B) Percent of wild-type female mosquitoes responding to varying sensory cues (n = 5, $p < 0.0001$).

(C) Percent of female mosquitoes of indicated genotypes blood feeding in the presence of CO_2, human odor, and heat cues ($p < 0.0001$, n = 7–10).

(D) Percent of female mosquitoes of indicated genotypes blood feeding in the presence of CO_2 and heat cues, without human odor (n = 7, $p = 0.468$).

(E) Percent of female mosquitoes of indicated genotypes blood feeding in the presence of human-odor and heat cues without added CO_2 (n = 5–6; $p = 0.855$).

(F) Percent of female mosquitoes of indicated genotypes blood feeding in the presences of human-odor and CO_2 cues without heat cue (n = 6; $p = 0.944$). For the dot plots in (B)–(F), long lines represent the mean and short lines represent standard error. Statistical analysis was done using one-way ANOVA with post hoc Tukey's HSD test. Genotypes marked with different letters are significantly different. Human odor was collected from subject 1; see Table S2.

from assays that contain heated blood and CO_2 (Figures 3C and 3D), we hypothesize that the defect found in *Ir8a* mutants is due to human-odor detection.

Ae. aegypti IR8a Pathway Is Required to Detect Humans and Human Odor

We subsequently investigated whether the electrophysiological and behavioral defects recorded in *Ir8a* mutants could translate into impaired responses to human hosts. Using a uniport olfactometer with carbon-filtered air flow and added CO_2, we examined the attraction rate of olfactory receptor mutants to 15 different human subjects (Figure 4A; Table S1). Each subject was tested twice with wild-type (+/+), heterozygous ($Ir8a^{dsRED}$/+), *Ir8a* mutant ($Ir8a^{dsRED/dsRED}$), heteroallelic *Ir8a* mutant ($Ir8a^{attP/dsRED}$), *orco* mutant ($orco^{16/16}$), heteroallelic *orco* mutant ($orco^{5/16}$), and double-mutant ($Ir8a^{dsRED/dsRED}$, $orco^{16/16}$) female mosquitoes. In these assays, wild-type mosquitoes and *orco* mutants showed robust attraction. In contrast, attraction to humans was significantly impaired in *Ir8a* mutants (Figure 4B). Differences in attraction were significant for both genotype and the 15 human subjects tested (two-way ANOVA, $p < 0.0001$ for genotype and $p = 0.0095$ for subject). The statistical difference in mosquito attraction to individual human subjects reflects the differences in attractive cues that emanate from each subject. Surprisingly, the additional loss of *orco* in the double mutants did not significantly enhance the *Ir8a* human-detection defect in this assay (Figure 4B). This suggests the existence of other olfactory receptors that can respond to human odor, since the double mutant still retains some attraction.

We next asked if the loss of attraction was dependent on olfactory cues from human hosts or on other cues emanating from live humans, such as body heat, moisture, or visual cues. To test this, we excluded these other cues by trapping human odor on nylon sleeves previously worn by a human subject for 12 h and exposing the scented sleeves to mosquitoes in our uniport assay (Figure 4D). In order to ascertain how long the scented sleeves could continue to elicit attraction, we tested the responses of wild-type mosquitoes. Even after 7 trials, which take approximately 85 min to perform, we found no significant difference in attraction rate (Figure S3). Thus, a given scented nylon sleeve was never used for more than 7 consecutive trials. Nevertheless, we randomly tested all genotypes to control for any potential bias linked to the time at which the human odor was presented. Robust attraction was recorded in the wild-type, heterozygous controls, and *orco* mutants when the human-scented sleeve was simultaneously presented with CO_2. Consistent with the study carried out with human subjects, *Ir8a* mutants show deficits in detecting nylon sleeves perfumed with human odor in these assays (Figure 4E). The weak attraction in the mutants

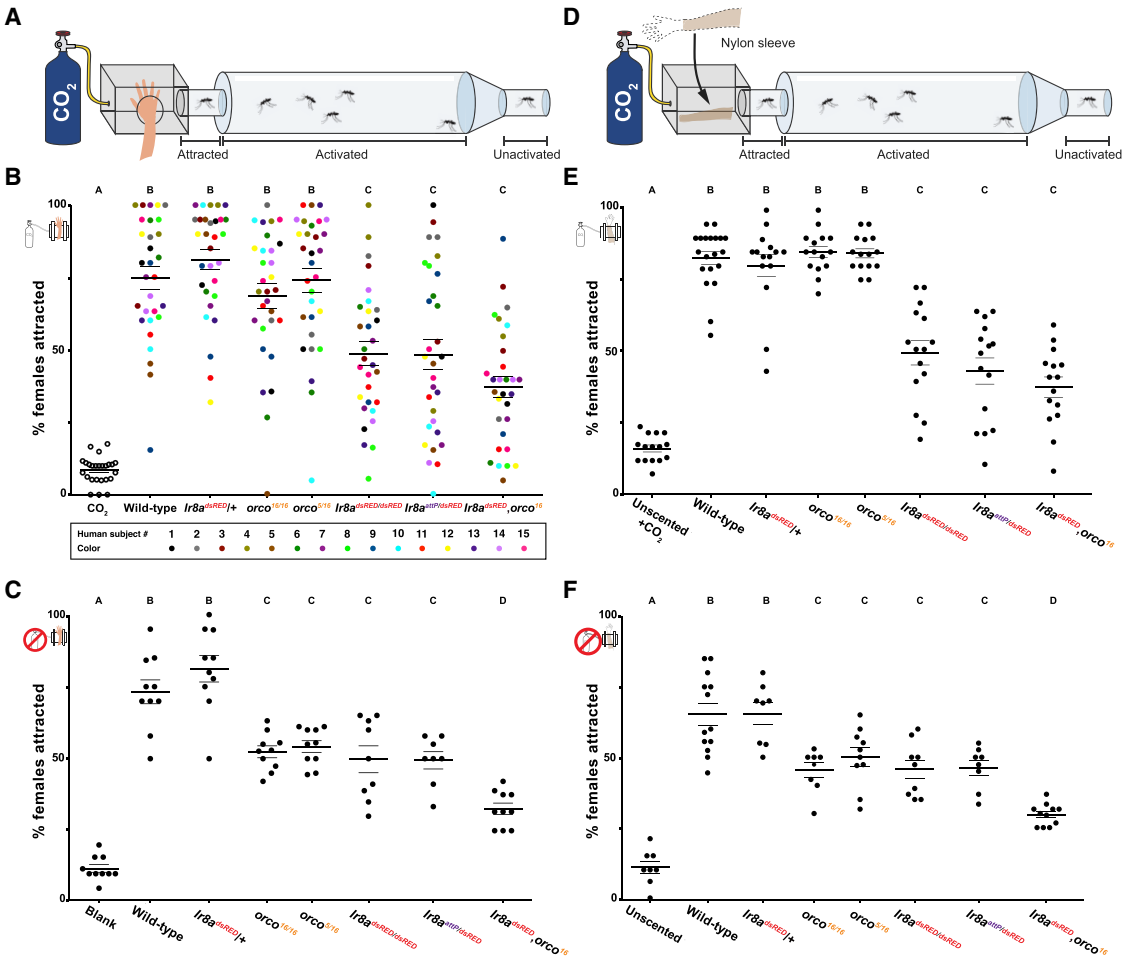

Figure 4. *Ae. aegypti* IR8a Pathway Is Required to Detect Humans and Human Odor

(A) Illustration showing mosquito attraction to a human arm in a uniport olfactometer.

(B) Dot plot of percent of female mosquitoes of indicated genotypes attracted to 15 human subjects in the presence of CO_2. Each subject was tested twice. An analysis was done using two-way ANOVA to compare the mean difference in attraction between subjects ($n = 30$, $p < 0.0001$) and genotypes ($n = 30$, $p < 0.0095$). Human subjects (1–15) were differentiated on the plots by dot color in this figure (bottom panel).

(C) Percent of female mosquitoes of indicated genotypes attracted to a human arm in the absence of CO_2 ($p < 0.0001$; $n = 8$–10).

(D) Illustration showing mosquito attraction to a human-scented nylon sleeve in a uniport olfactometer.

(E) Percent of female mosquitoes of indicated genotypes attracted to human odor trapped on nylon sleeve in the presence of CO_2. Data was analyzed using one-way ANOVA ($n = 15$, $p = 0.0001$).

(F) Percent of female mosquitoes of indicated genotypes attracted to human odor trapped on nylon sleeve in the absence of CO_2 ($p = 0.0001$; $n = 15$). For the dot plots, long lines represent the mean, and short lines represent standard error. All data above was analyzed using one-way ANOVA. Genotypes marked with different letters are significantly different by post hoc Tukey's HSD test. Human subject 1 was used in the experiments in panels (C), (E), & (F). See also Figures S3 and S4 as well as Table S2.

cannot be explained by a defect in locomotion or overall fitness of the *Ir8a* mutants (Figures S2A–S2F). This suggests that an impairment in sensitivity to *Ir8a*-dependent odor ligands presented by humans is responsible for the behavioral defect seen in the uniport olfactometer assays with human subjects.

CO_2 Differentially Modulates the IR8a and Orco Pathways

We asked if CO_2 activation can modulate the attraction rate of *Ir8a* mutants by testing the attraction of the mutants to a human subject without including added CO_2 in the assay. In contrast to uniport assays that included CO_2 (Figures 4B and 4E), we recorded a host-seeking deficit in *orco* mutants in the absence of added CO_2 that was not statistically different than *Ir8a* mutants (Figures 4C and 4F). This supports an earlier study that reported that CO_2 synergizes with human odor to rescue host-seeking defects in *orco* mutants [21]. Similar to what was observed with a human host when CO_2 is not included in the assay, both *Ir8a* and *orco* single mutants lose strong attraction to nylon sleeves perfumed with human odor compared to wild-type controls (Figures 4C and 4F). In contrast to *orco* mutants, *Ir8a* mutants' response to human odor was not changed by the presence or absence of CO_2 (Figure S4A). We found no difference in CO_2 levels in the uniport when airflow is

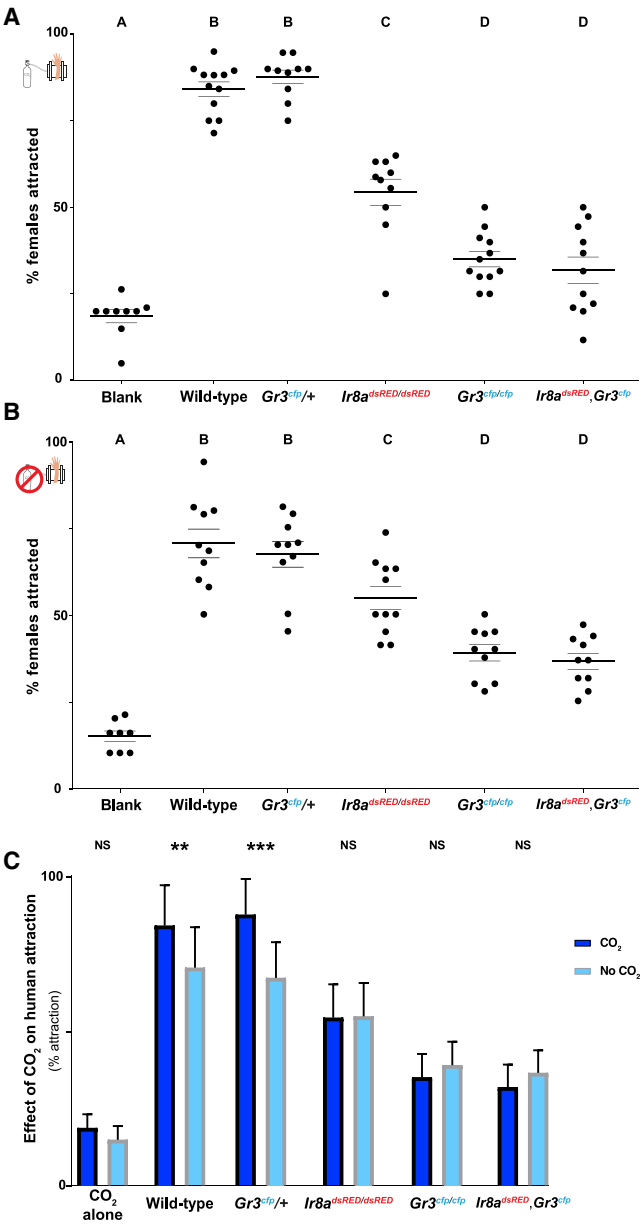

Figure 5. The Loss of *Gr3* Enhances the *Ir8a*-Dependent Host-Seeking Defect

(A) Percent of female mosquitoes of indicated genotypes attracted to a human arm in the presence of CO_2 ($p < 0.0001$; n = 10–12).

(B) Percent of female mosquitoes of indicated genotypes attracted to a human arm in the absence of CO_2 ($p < 0.0001$; n = 9–11). Analysis was done using one-way ANOVA by comparing mean attraction across all genotypes. Genotypes marked with different letters are significantly different by post hoc Tukey's HSD test. For the dot plots in (A) and (B), long lines represent the mean, and short lines represent standard error.

(C) Percentage response of mosquitoes attracted to humans in the presence and absence of CO_2 represented on a bar plot showing mean and standard error. Data compared in (C) are from Figures 5A and 5B. Genotypes were analyzed by two-way ANOVA with grouped column statistics ($p < 0.001$). Genotypes marked with asterisks are significantly different. Human subject 1 was used in the experiments in this figure. See also Figure S4 and Table S2.

or is not co-presented with a human arm (Figure S4B). Passing airflow over a human arm in the presence of CO_2 did not increase CO_2 levels versus airflow and CO_2 alone (Figure S4B).

Similar to what was observed in Figure 4C, attraction to human-scented nylon sleeves is impaired in *Ir8a*^{dsRED}, *orco*[16] double mutants when CO_2 is absent (Figure 4F). As the genetic interaction between *Ir8a* and *orco* is dependent on CO_2 sensation, we hypothesize that CO_2 can activate additional olfactory receptor pathways that integrate the response to host odor cues in the absence of the OR pathway. Unlike that in *orco* mutants, the response of *Ir8a* mutants to human odor is not modulated by CO_2 (Figures 4C and S4A). This suggests that CO_2 sensitization and host odor detection by other olfactory receptor pathways are not sufficient to rescue the *Ir8a* host-seeking defect. To explore this difference, we tested the genetic interaction between *Ir8a* and *Gr3* mutants.

The Loss of *Gr3* Enhances the *Ir8a*-Dependent Host-Seeking Defect

The integration of host cues requires CO_2 and is dependent on *Gr3* in *Ae. aegypti* [22]. We investigated whether *Ir8a* and *Gr3* act together to drive host attraction. Using our uniport assay with a human host and added CO_2, we found that host-seeking behavior is also impaired not only in the *Ir8a* mutants but also in the *Gr3* mutants (Figure 5A). The loss of *Gr3* function causes a stronger reduction in host-seeking behavior than does the loss of *Ir8a* function (Figures 5A and 5B). The loss of both *Ir8a* and *Gr3* causes a host-seeking defect similar to that caused by the loss of *Gr3* alone (Figures 5A and 5B). This suggests that *Gr3* may be necessary for *Ir8a* function. Unlike that of *orco* mutants or wild-type controls, the attraction rate of *Ir8a* mutants was not modified when CO_2 was excluded from olfactometer assays with human odor (Figures 5C and S4A). Therefore, CO_2 activation is not sufficient to rescue the *Ir8a* host-seeking phenotype. This suggests that detection of *Ir8a*-dependent ligands, unlike *orco*-dependent ligands, is a non-redundant component of mosquito host detection.

DISCUSSION

Here, we present evidence that strongly suggests that *Ir8a* is a crucial mediator of *Ae. aegypti* mosquito attraction to humans and human odor. *Ir8a* is necessary for the electrophysiological response of the mosquito antennae to acidic volatiles found in human odor, including lactic acid. We present evidence that the *Ae. aegypti* IR8a pathway responds to human-odor cues during blood feeding and enables mosquito attraction to humans, human odor, and lactic acid. By varying CO_2 in our behavioral assays and testing the genetic interactions between *Ir8a* and *orco* as well as *Ir8a* and *Gr3*, we have connected the *Ir8a* pathway to the overall integration of host cues by mosquitoes. Taken together, our evidence supports the conclusion that the *Ir8a* pathway is a key participant in the multimodal integration of host-odor cues by *Ae. aegypti* mosquitoes, whose absence cannot be compensated for by other olfactory receptors.

Lactic acid and carboxylic acids are a major component of human sweat and may distinguish humans from other vertebrate hosts [31]. Lactic acid acts synergistically with certain volatile compounds to increase mosquito attraction. Our results support the conclusion that the detection of lactic acid and carboxylic

acids by mosquitoes is necessary for robust attraction to humans. Further study will be required to determine whether *Ir8a* mediates the decision to target humans over other vertebrate hosts. In addition, the identification of IR8a as a co-receptor required for lactic acid detection allows for the identification of the odor-tuned receptor(s) that are necessary to sense this important kairomone.

Our results have implications not only for IRs but also for how sensory information from the OR and the CO_2-sensing GR pathways are integrated during mosquito host detection. Our experiments reveal that *Ir8a* and *Gr3* are both required for human host detection, but the genetic interaction of the two genes is not additive. It could have been possible that the loss of both genes could eliminate mosquito host detection, but this was not the case. Double mutants lacking *Ir8a* and *Gr3* show a significant reduction in host detection when compared to *Ir8a* mutants alone (Figures 5A and 5B). However, the defects in the double mutant are not enhanced when compared to those in *Gr3* mutants with an intact *Ir8a* gene (Figures 5A and 5B). In addition, the phenotype of *Ir8a* mutants is not rescued by the presence of CO_2 (Figures 5C and S4A). This suggests that *Gr3* activation is necessary but not sufficient to promote *Ir8a*-dependent host attraction. *Gr3* activation by CO_2 may make acidic volatiles in human odor salient to the mosquito, but *Ir8a* is still required to detect these odors.

Our evidence suggests that *Gr3* activation gates the responses of both the OR pathway and the IR8a pathway to promote host seeking, but how this interaction is achieved is not the same. Based on our results, the loss of *Ir8a* cannot be compensated for by using other olfactory receptors as in *orco* mutants. Our genetic interaction experiments support the conclusion that *Gr3* activation is required for IR8a pathway function, and CO_2-dependent gating of additional *Ir8a*-independent receptors can compensate for the loss of *orco* function. The identification of these receptors is imperative for understanding how mosquitoes finds their human hosts.

The functional characterization of an ionotropic chemoreceptor family member in *Ae. aegypti* we present provides insight into how olfactory receptor pathways can interact to mediate the detection of humans and their odor by mosquitoes. However, the understanding of how these sensory responses are integrated to facilitate host detection is far from complete. Determining whether the integration of cues occurs within the antennal lobe or in higher olfactory processing centers in the brain will help reveal the dynamics of the innate neural circuits that enable mosquito host detection. Further study is necessary to uncover how mosquitoes sense their human hosts, from the peripheral perception of cues to the integration and processing of the information in the central nervous system, and, finally, to the motor circuit outputs that drive host-seeking behavior.

STAR★METHODS

Detailed methods are provided in the online version of this paper and include the following:

SUPPLEMENTAL INFORMATION

Supplemental Information can be found with this article online at https://doi.org/10.1016/j.cub.2019.02.045.

A video abstract is available at https://doi.org/10.1016/j.cub.2019.02.045#mmc5.

ACKNOWLEDGMENTS

We would like to thank Leslie Vosshall for her support of the project and her comments on the figures. We are so grateful to André Luis da Costa da Silva, Marcela Nouzova, Fernando Noriega, Phillip Stoddard, Elina Barredo, Emily Dennis, Trevor Sorrells, Maria Elena de Obaldia, and Michael Sheriff for their comments and suggestions on the manuscript. We are grateful to Robert Harrell II and the Insect Transformation Facility at the University of Maryland for injecting mosquito embryos with CRISPR/Cas9 reagents. We appreciate Jeremy Wood's useful suggestions on the Graphical Abstract design. This work was supported by the National Institute of Allergy and Infectious Diseases of the National Institutes of Health under award number 1K22AI112585-01 and startup funds from Florida International University. M.D. was also supported by the Centers for Disease Control and Prevention (CDC) Southeastern Center of Excellence in Vector Borne Diseases. The content is solely the responsibility of the authors and does not necessarily represent the official views of the National Institutes of Health or the CDC.

AUTHOR CONTRIBUTIONS

M.D. conceived and supervised the study and generated the *Ir8a* mutants. J.I.R. performed experiments and maintained mutant lines with S.G., V.S., and J.S.C. N.M. and M.C.S. performed the electrophysiology experiments and provided feedback on the manuscript. M.D. and J.S.C. created the graphical abstract. M.D., J.S.C., M.C.S., and J.I.R. made the figures. M.D. and J.I.R wrote the manuscript.

DECLARATION OF INTERESTS

The authors declare no competing interests.

Received: October 30, 2018
Revised: January 16, 2019
Accepted: February 19, 2019
Published: March 28, 2019

REFERENCES

1. Petersen, L.R., Jamieson, D.J., Powers, A.M., and Honein, M.A. (2016). Zika Virus. N. Engl. J. Med. *374*, 1552–1563.
2. Raji, J.I., and DeGennaro, M. (2017). Genetic analysis of mosquito detection of humans. Curr. Opin. Insect Sci. *20*, 34–38.
3. Takken, W., and Knols, B.G. (1999). Odor-mediated behavior of Afrotropical malaria mosquitoes. Annu. Rev. Entomol. *44*, 131–157.
4. Verhulst, N.O., Qiu, Y.T., Beijleveld, H., Maliepaard, C., Knights, D., Schulz, S., Berg-Lyons, D., Lauber, C.L., Verduijn, W., Haasnoot, G.W., et al. (2011). Composition of human skin microbiota affects attractiveness to malaria mosquitoes. PLoS ONE *6*, e28991.
5. Acree, F., Jr., Turner, R.B., Gouck, H.K., Beroza, M., and Smith, N. (1968). L-Lactic acid: a mosquito attractant isolated from humans. Science *161*, 1346–1347.
6. Davis, E.E., and Sokolove, P.G. (1976). Lactic acid-sensitive receptors on the antennae of the mosquito, *Aedes aegypti*. J. Comp. Physiol. *105*, 43–54.
7. Braks, M.A.H., Meijerink, J., and Takken, W. (2001). The response of the malaria mosquito, *Anopheles gambiae*, to two components of human sweat, ammonia and l-lactic acid, in an olfactometer. Physiol. Entomol. *26*, 142–148.
8. Smallegange, R.C., Qiu, Y.T., Bukovinszkiné-Kiss, G., Van Loon, J.J.A., and Takken, W. (2009). The effect of aliphatic carboxylic acids on olfaction-based host-seeking of the malaria mosquito *Anopheles gambiae sensu stricto*. J. Chem. Ecol. *35*, 933–943.
9. Majeed, S., Hill, S.R., Birgersson, G., and Ignell, R. (2016). Detection and perception of generic host volatiles by mosquitoes modulate host preference: context dependence of (*R*)-1-octen-3-ol. R. Soc. Open Sci. *3*, 160467.
10. Pitts, R.J., Derryberry, S.L., Zhang, Z., and Zwiebel, L.J. (2017). Variant ionotropic receptors in the malaria vector mosquito *Anopheles gambiae* tuned to amines and carboxylic acids. Sci. Rep. *7*, 40297.
11. Hansson, B.S., and Stensmyr, M.C. (2011). Evolution of insect olfaction. Neuron *72*, 698–711.
12. Vosshall, L.B., Amrein, H., Morozov, P.S., Rzhetsky, A., and Axel, R. (1999). A spatial map of olfactory receptor expression in the *Drosophila* antenna. Cell *96*, 725–736.
13. Bohbot, J., Pitts, R.J., Kwon, H.-W., Rützler, M., Robertson, H.M., and Zwiebel, L.J. (2007). Molecular characterization of the *Aedes aegypti* odorant receptor gene family. Insect Mol. Biol. *16*, 525–537.
14. Benton, R., Vannice, K.S., Gomez-Diaz, C., and Vosshall, L.B. (2009). Variant ionotropic glutamate receptors as chemosensory receptors in *Drosophila*. Cell *136*, 149–162.
15. Jones, W.D., Cayirlioglu, P., Kadow, I.G., and Vosshall, L.B. (2007). Two chemosensory receptors together mediate carbon dioxide detection in *Drosophila*. Nature *445*, 86–90.
16. Kwon, J.Y., Dahanukar, A., Weiss, L.A., and Carlson, J.R. (2007). The molecular basis of CO_2 reception in *Drosophila*. Proc. Natl. Acad. Sci. USA *104*, 3574–3578.
17. Lu, T., Qiu, Y.T., Wang, G., Kwon, J.Y., Rutzler, M., Kwon, H.-W., Pitts, R.J., van Loon, J.J.A., Takken, W., Carlson, J.R., and Zwiebel, L.J. (2007). Odor coding in the maxillary palp of the malaria vector mosquito *Anopheles gambiae*. Curr. Biol. *17*, 1533–1544.
18. Benton, R., Sachse, S., Michnick, S.W., and Vosshall, L.B. (2006). Atypical membrane topology and heteromeric function of *Drosophila* odorant receptors in vivo. PLoS Biol. *4*, e20.
19. Sato, K., Pellegrino, M., Nakagawa, T., Nakagawa, T., Vosshall, L.B., and Touhara, K. (2008). Insect olfactory receptors are heteromeric ligand-gated ion channels. Nature *452*, 1002–1006.
20. Butterwick, J.A., Del Mármol, J., Kim, K.H., Kahlson, M.A., Rogow, J.A., Walz, T., and Ruta, V. (2018). Cryo-EM structure of the insect olfactory receptor Orco. Nature *560*, 447–452.
21. DeGennaro, M., McBride, C.S., Seeholzer, L., Nakagawa, T., Dennis, E.J., Goldman, C., Jasinskiene, N., James, A.A., and Vosshall, L.B. (2013). *orco* mutant mosquitoes lose strong preference for humans and are not repelled by volatile DEET. Nature *498*, 487–491.
22. McMeniman, C.J., Corfas, R.A., Matthews, B.J., Ritchie, S.A., and Vosshall, L.B. (2014). Multimodal integration of carbon dioxide and other sensory cues drives mosquito attraction to humans. Cell *156*, 1060–1071.
23. Silbering, A.F., Rytz, R., Grosjean, Y., Abuin, L., Ramdya, P., Jefferis, G.S.X.E., and Benton, R. (2011). Complementary function and integrated wiring of the evolutionarily distinct *Drosophila* olfactory subsystems. J. Neurosci. *31*, 13357–13375.
24. Abuin, L., Bargeton, B., Ulbrich, M.H., Isacoff, E.Y., Kellenberger, S., and Benton, R. (2011). Functional architecture of olfactory ionotropic glutamate receptors. Neuron *69*, 44–60.
25. Matthews, B.J., McBride, C.S., DeGennaro, M., Despo, O., and Vosshall, L.B. (2016). The neurotranscriptome of the *Aedes aegypti* mosquito. BMC Genomics *17*, 32.
26. Matthews, B.J., Dudchenko, O., Kingan, S.B., Koren, S., Antoshechkin, I., Crawford, J.E., Glassford, W.J., Herre, M., Redmond, S.N., Rose, N.H., et al. (2018). Improved reference genome of *Aedes aegypti* informs arbovirus vector control. Nature *563*, 501–507.
27. Ai, M., Min, S., Grosjean, Y., Leblanc, C., Bell, R., Benton, R., and Suh, G.S.B. (2010). Acid sensing by the *Drosophila* olfactory system. Nature *468*, 691–695.
28. Ai, M., Blais, S., Park, J.-Y., Min, S., Neubert, T.A., and Suh, G.S.B. (2013). Ionotropic glutamate receptors IR64a and IR8a form a functional odorant receptor complex in vivo in *Drosophila*. J. Neurosci. *33*, 10741–10749.
29. Carey, A.F., Wang, G., Su, C.-Y., Zwiebel, L.J., and Carlson, J.R. (2010). Odorant reception in the malaria mosquito *Anopheles gambiae*. Nature *464*, 66–71.
30. Hussain, A., Zhang, M., Üçpunar, H.K., Svensson, T., Quillery, E., Gompel, N., Ignell, R., and Grunwald Kadow, I.C. (2016). Ionotropic chemosensory receptors mediate the taste and smell of polyamines. PLoS Biol. *14*, e1002454.
31. Dekker, T., Steib, B., Cardé, R.T., and Geier, M. (2002). L-lactic acid: a human-signifying host cue for the anthropophilic mosquito *Anopheles gambiae*. Med. Vet. Entomol. *16*, 91–98.
32. Zhang, Y.V., Ni, J., and Montell, C. (2013). The molecular basis for attractive salt-taste coding in *Drosophila*. Science *340*, 1334–1338.
33. Chen, C., Buhl, E., Xu, M., Croset, V., Rees, J.S., Lilley, K.S., Benton, R., Hodge, J.J.L., and Stanewsky, R. (2015). *Drosophila* Ionotropic Receptor 25a mediates circadian clock resetting by temperature. Nature *527*, 516–520.
34. Enjin, A., Zaharieva, E.E., Frank, D.D., Mansourian, S., Suh, G.S.B., Gallio, M., and Stensmyr, M.C. (2016). Humidity Sensing in *Drosophila*. Curr. Biol. *26*, 1352–1358.
35. Knecht, Z.A., Silbering, A.F., Ni, L., Klein, M., Budelli, G., Bell, R., Abuin, L., Ferrer, A.J., Samuel, A.D., Benton, R., and Garrity, P.A. (2016). Distinct combinations of variant ionotropic glutamate receptors mediate thermosensation and hygrosensation in *Drosophila*. eLife *5*, 44.
36. Knecht, Z.A., Silbering, A.F., Cruz, J., Yang, L., Croset, V., Benton, R., and Garrity, P.A. (2017). Ionotropic Receptor-dependent moist and dry cells control hygrosensation in *Drosophila*. eLife *6*, 44.
37. Silbering, A.F., Bell, R., Münch, D., Cruchet, S., Gomez-Diaz, C., Laudes, T., Galizia, C.G., and Benton, R. (2016). Ir40a neurons are not DEET detectors. Nature *534*, E5–E7.
38. Ahn, J.-E., Chen, Y., and Amrein, H. (2017). Molecular basis of fatty acid taste in *Drosophila*. eLife *6*, e30115.
39. Chen, Y., and Amrein, H. (2017). Ionotropic receptors mediate *Drosophila* oviposition preference through sour gustatory receptor neurons. Curr. Biol. *27*, 2741–2750.e4.
40. van Breugel, F., Huda, A., and Dickinson, M.H. (2018). Distinct activity-gated pathways mediate attraction and aversion to CO_2 in Drosophila. Nature *564*, 420–424.

41. Pitts, R.J., Rinker, D.C., Jones, P.L., Rokas, A., and Zwiebel, L.J. (2011). Transcriptome profiling of chemosensory appendages in the malaria vector *Anopheles gambiae* reveals tissue- and sex-specific signatures of odor coding. BMC Genomics *12*, 271.

42. Rinker, D.C., Zhou, X., Pitts, R.J., Rokas, A., and Zwiebel, L.J.; AGC Consortium (2013). Antennal transcriptome profiles of anopheline mosquitoes reveal human host olfactory specialization in *Anopheles gambiae*. BMC Genomics *14*, 749.

43. Kistler, K.E., Vosshall, L.B., and Matthews, B.J. (2015). Genome engineering with CRISPR-Cas9 in the mosquito *Aedes aegypti*. Cell Rep. *11*, 51–60.

44. Zhang, X.-H., Tee, L.Y., Wang, X.-G., Huang, Q.-S., and Yang, S.-H. (2015). Off-target effects in CRISPR/Cas9-mediated genome engineering. Mol. Ther. Nucleic Acids *4*, e264.

45. Ja, W.W., Carvalho, G.B., Mak, E.M., de la Rosa, N.N., Fang, A.Y., Liong, J.C., Brummel, T., and Benzer, S. (2007). Prandiology of *Drosophila* and the CAFE assay. Proc. Natl. Acad. Sci. USA *104*, 8253–8256.

46. Liesch, J., Bellani, L.L., and Vosshall, L.B. (2013). Functional and genetic characterization of neuropeptide Y-like receptors in *Aedes aegypti*. PLoS Negl. Trop. Dis. *7*, e2486.

47. Bernier, U.R., Kline, D.L., Posey, K.H., Booth, M.M., Yost, R.A., and Barnard, D.R. (2003). Synergistic attraction of *Aedes aegypti* (L.) to binary blends of L-lactic acid and acetone, dichloromethane, or dimethyl disulfide. J. Med. Entomol. *40*, 653–656.

48. Hallem, E.A., Ho, M.G., and Carlson, J.R. (2004). The molecular basis of odor coding in the *Drosophila* antenna. Cell *117*, 965–979.

49. Couto, A., Alenius, M., and Dickson, B.J. (2005). Molecular, anatomical, and functional organization of the *Drosophila* olfactory system. Curr. Biol. *15*, 1535–1547.

50. Benton, R., and Dahanukar, A. (2011). Electrophysiological recording from *Drosophila* olfactory sensilla. Cold Spring Harb. Protoc. *2011*, 824–838.

51. Cosgrove, J.B., and Wood, R.J. (1995). Probing and gorging responses of three mosquito species to a membrane feeding system at a range of temperatures. J. Am. Mosq. Control Assoc. *11*, 339–342.

52. Hwang, W.Y., Fu, Y., Reyon, D., Maeder, M.L., Tsai, S.Q., Sander, J.D., Peterson, R.T., Yeh, J.R., and Joung, J.K. (2013). Efficient genome editing in zebrafish using a CRISPR-Cas system. Nat. Biotechnol. *31*, 227–229.

53. Corfas, R.A., and Vosshall, L.B. (2015). The cation channel TRPA1 tunes mosquito thermotaxis to host temperatures. eLife *4*, e11750.

54. Livak, K.J., and Schmittgen, T.D. (2001). Analysis of relative gene expression data using real-time quantitative PCR and the 2(-Delta Delta C(T)) Method. Methods *25*, 402–408.

STAR★METHODS

KEY RESOURCES TABLE

REAGENT or RESOURCE	SOURCE	IDENTIFIER
Chemicals, Peptides, and Recombinant Proteins		
Geranylacetone	Sigma-Aldrich	C.A.S. 689-67-8
Methyl-5-hepten-2-one	Sigma-Aldrich	C.A.S. 110-93-0
Dodecanal	Sigma-Aldrich	C.A.S. 112-54-9
L-Lactic acid	Sigma-Aldrich	C.A.S. 79-33-4
Octanoic acid	ICN	C.A.S. 124-07-2
Heptanoic acid	ICN	C.A.S. 111-14-8
Butyric acid	ICN	C.A.S. 107-92-6
Octanal	Chemicon:Acros	C.A.S. 124-13-0
Nonanal	Chemicon:Acros	C.A.S. 124-19-6
Limonene	Fluka	C.A.S. 5989-27-5
Nonanoic acid	Fluka	C.A.S. 112-05-0
2-ethyl hexanol	Lancaster	C.A.S. 104-76-7
1-octen-3-ol	Janssen Chimica	C.A.S. 3391-86-4
Guanidine thiocyanate	Sigma-Aldrich	C.A.S. 593-84-0
Sarkosyl	Fisher Scientific	C.A.S. 137-16-6
Chloroform	Fisher Scientific	C.A.S. 67-66-3
Linalool	Sigma-Aldrich	C.A.S. 78-70-6
2-mercapthoethanol	Sigma-Aldrich	C.A.S: 60-24-2
Restriction Enzymes		
PmeI	New England Biolabs	Catalog # R0560S
EcoRI	New England Biolabs	Catalog # R0101S
XhoI	New England Biolabs	Catalog # R0146S
MluI	New England Biolabs	Catalog # R1089S
Recombinant DNA		
pGT-Ir8a (used for donor plasmid)	This study	N/A
pMLM3613 (used for Cas9 MRNA)	[52]	Addgene # 42251
pSL1180:polyUBdsRED (donor plasmid)	[53]	Addgene # 49327
Oligonucleotides (primers)	Integrated DNA Technologies	See Table S1
Critical Commercial Assays		
MEGAscript T7 Transcription Kit	Life Technologies	Catalog # AM1334
MEGAclear transcription clean-up kit	Life Technologies	Catalog # AM1908
mMachine mMachine T7 ultra kit	Thermo-Fisher Scientific	Catalog # AM1345
DNeasy blood & tissue kits	QIAGEN GmbH	Catalog # 69504
NucleoSpin gel and PCR cleanup kit	Machery-Nagel Inc.	Catalog # 740609
NEB PCR cloning kit	New England Biolabs	Catalog # E1202S
RNAlater stablization solution	Invitrogen	Catalog # AM7020
RNAid Kit	MPBio	Catalog # 111007200
TURBO DNA-free kit	Invitrogen	Catalog # AM1907
KOD polymerase	EMD Millipore	Catalog # 71086
Qiaquick PCR purification kit	QIAGEN	Catalog # 28106
Infusion HD cloning kit	Clontech	Catalog # 638909
QIAGEN Endo-free Maxiprep kit	QIAGEN	Catalog #12362
SimpleSeq premixed kit	Eurofins	N/A
IBI Genomic DNA extraction kit	IBI scientific	Catalog # IB47222

(*Continued on next page*)

Continued

REAGENT or RESOURCE	SOURCE	IDENTIFIER
Amplitaq Gold 360 PCR master mix	Applied Biosystems	Catalog # 4398881
QIAEX II Gel extraction kit	QIAGEN GmbH	Catalog # 20051
pCR2.1 TOPO TA vector	Invitrogen	Catalog # K462040
One Shot TOP10 cells	Invitrogen	Catalog # C607003
QIAprep Spin Miniprep kit	QIAGEN GmbH	Catalog # 27104
SuperScript II RT reagent kit	Invitrogen	Catalog # 18080-051
RNase cocktail enzyme mix	Thermo-Fisher Scientific	Catalog # AM2286
TaqMan 2X universal master mix	Thermo-Fisher Scientific	Catalog # 4324018
Custom TaqMan Ir8a probe	ThermoFisher Scientific	Catalog # 4331348
Experimental Models: Organisms/Strains		
Ae. aegypti: Orlando	Leslie Vosshall	N/A
Ae. aegypti: $Ir8a^{dsRED}$	This study	N/A
Ae. aegypti: $Ir8a^{attP}$	This study	N/A
Ae. aegypti: $Orco^{5}$	[21], BEI resources	NR-44377
Ae. aegypti: $Orco^{16}$	[21], BEI resources	NR-44378
Ae. aegypti: $Gr3^{cf.p}$	[22], BEI resources	NR-48760
Software and Algorithms		
Syntech EAG-Pro 4.6	Custom-made	N/A
Peak Scanner software	Applied Biosystems	v1.0
Impedance amplifier	Syntech	IDAC-4
ZiFit	https://zifit.partners.org/ZiFit/	N/A
Real time PCR system	Applied Biosystems	7500
Locomotor activity monitor	Trikinetics Inc.	LAM 25
SnapGene & SnapGene Viewer	SnapGene	N/A
SDS software	Applied Biosystems	v1.4.1
GraphPad Prism	GraphPad	Prism v7 & v8
Other		
Tetramin tropical fish food	Tetra	Catalog # 16152
Capillary tubes	Blaubrand Intramark	Catalog # 1904637
Cellulose acetate fly vial plug	Genesee Scientific	Catalog # 49-101
CO_2 diffusion pad	Tritech Research	Model # MINJ-DROS-FP
Membrane feeders	Chemglass	Catalog # CG-1835-70
Uniport olfactometer	Custom-made	N/A
Carbon dioxide monitor	Amprobe	Catalog # CO2-100
Acrylic flowmeter	Dwyer Instrument Inc.	Catalog # VFA-4-SSV
Suntan knee-high pantyhose	L'eggs brand, Hanes	Model # 39400
Disposable pellet pestles	Fisher Scientific	Catalog # 12-141-364

CONTACT FOR REAGENT AND RESOURCE SHARING

Further information and requests for resources and reagents should be directed to and will be fulfilled by the Lead Contact, Matthew DeGennaro (mdegenna@fiu.edu).

EXPERIMENTAL MODEL AND SUBJECT DETAILS

Statement of Research Ethics

All research was conducted in compliance with the NIH guidelines and the Florida International University Environmental Health and Safety guideline. Laboratory practices, facilities and equipment were reviewed and approved by the Florida International University Institutional Biosafety Committee (IBC-18-004) and Institutional Review Board (IRB-16-0388 & IRB-16-0386-CR02). Informed consent was obtained from human subject volunteers before their participation in this study.

Insect rearing

Aedes aegypti mosquitoes were reared and maintained at 25-28°C, 75% relative humidity under a 14:10 light-dark cycle (lights on at 8 am). All mosquitoes used in these experiments were generated from the Orlando laboratory strain. Mosquito eggs were hatched in deionized, deoxygenated water containing dissolved tablets of Tetramin tropical fish food (catalog #16152, Tetra, Melle, Germany), which served as food for the emerged larvae. Adult mosquitoes were given *ad libitum* access to 10% sucrose solution. About 1 to 2-week-old adult females were fed on defibrinated sheep blood to generate eggs. Before behavioral assays, 5 to 7 day old sugar-fed mosquitoes were sorted and sexed under hypothermic (4°C) conditions and fasted for up to 24 hours on water. All mosquitoes were tested only once in the behavioral assays in this study and then sacrificed.

Subject volunteers

A total of 18 human subject volunteers participated in host seeking experiments (Table S2). However, three subjects were later excluded because they failed either, to complete all the trials or their body odor was not attractive to wild-type mosquitoes. Each subject was tested twice to assess their attractiveness to mosquitoes. The volunteers were diverse in age (19 to 41 years), sex (Male = 7, Female = 8), and race (White = 5, Hispanic = 7, Asian = 1, Black = 2).

METHOD DETAILS

CRISPR/Cas9 nuclease reagents

CRISPR short guided RNAs (sgRNA) were designed according to standard protocols [43]. The sgRNAs sequences for the mutagenesis of exon 2 and exon 3 of *Ir8a* gene were chosen by the presence of protospacer-adjacent motifs (PAMs) with the sequence NGG. Generated sgRNA sequences were checked for potential off-target binding sites using ZiFit (http://zifit.partners.org/ZiFiT/). Double-stranded DNA templates for specific sgRNAs were produced by performing a template-free PCR with two overlapping oligonucleotides. One containing the specific target sequences (*Ir8a*^{dsRED} exon2: GGGCGGACAAAATGGCGTAT and *Ir8a*^{attP} exon 3: GGACATCTGTCGACGATAAC), and the universal CRISPR reverse primer (Table S1). The forward primers used were IR8aExon2CRISPRF and IR8aExon3CRISPRF. The reverse primer used was sgRNArev. Both sgRNAs were produced using MEGAscript T7 Transcription Kit (Catalog #AM1334, Life Technologies, Carlsbad, CA, USA). Following incubation, sgRNA transcripts were purified using MEGAclear Transcription Clean-Up Kit (Catalog #AM1908, Life Technologies) and verified on the Agilent bioanalyzer (Agilent, Santa Clara, CA, USA).

The Cas9 polyadenylated mRNA was made by digesting the MLM3613 plasmid [52] with the PmeI restriction enzyme (New England Biolabs, Ipswich, MA, USA), miniprep purifying the linearized plasmid, and *in vitro* transcribing the mRNA from the DNA fragment using the mMessage mMachine T7 ultra kit (Catalog #AM1345, Thermo Fisher Scientific). The mRNA transcript was purified using MEGAclear Transcription Clean-Up Kit (Catalog #AM1908, Life Technologies) and checked on the Agilent bioanalyzer (Agilent). MLM3613 was a gift from Keith Joung (Addgene plasmid #42251; http://www.addgene.org/42251/; RRID: Addgene_42251).

Donor DNAs

The single stranded oligo nucleotide (ssODN) used to integrate *attP* recombination site sequences into exon 3 of *Ir8a* was synthesized by Integrated DNA Technologies (www.idtdna.com) using the 20 nmole ultramer service with standard desalting. The ssODN contains a 50 bp *attP* site flanked by 75 bp of homologous sequences to the target site on both sides:

GATTCTCGGTTCTGGATGCCTGACGGCAGTCGAATGTTACGATACAATTTGAACGTTTCGATTTGGACATCTGTC**CTACGCCCCCAACTGAGAGAACTCAAAGGTTACCCCAGTTGGGGCACTAC**AACGGGTCTGCTGCAATACACCTTGGGACGATCGAGAAGGGTGATGTGGTACCGTTCGTGGGTCAGAAGATCAAA (*attP* sequence in bold).

To generate the donor DNA to integrate into exon 2 of IR8a, the pSL1180:polyUBdsRED [53] was modified to include homologous sequences surrounding the CRISPR target site. The 796 bp left arm and 1005 bp right arms were amplified from Orlando strain *Ae. aegypti* genomic DNA using Novagen KOD polymerase (EMD Millipore, Temecula, CA, USA) and these primers: infusionIR8LA_1, infusionIR8LA_2, infusion_IR8RA1, and infusion_IR8RA2 (Table S1).

After the PCR fragments were amplified and purified with Qiaquick PCR purification kit (Catalog #28106, QIAGEN, Hilgen, Germany), pSL 1180:polyUBdsRED was digested with both EcoRI and XhoI (New England Biolabs). The 3253 bp fragment (pSL 1180 backbone) and 2321 bp fragment (polyubiquitin:dsRED:SV40) were both gel purified. The left homologous arm PCR, polyubiquitin:dsRED fragment, the right homologous arm PCR, and psl1180 backbone were simultaneously assembled using a recombination based method, Infusion HD (Catalog #638909, Clontech). The resulting DNA was cut with the MluI restriction enzyme (New England Biolabs) and Sanger sequenced to confirm the proper integration of the fragments. The final plasmid DNA, pGT-Ir8a, was purified from *E. coli* using the QIAGEN Endo-free Maxiprep DNA (Catalog #12362, QIAGEN) isolation kit.

Ir8a^{dsRED} *and Ir8a*^{attP} mutant allele generation and detection

To generate stable germline mutations, CRISPR-Cas9 reagents were injected into the posterior end of the pre-blastoderm embryos. This stage allows nuclei that will become somatic and germline cells to be exposed to the CRISPR-Cas9 complex since the dividing nuclei have not yet undergone cytokinesis. Microinjection into *Ae. aegypti* pre-blastoderm embryos was performed at the Insect Transformation Facility at the University of Maryland. The microinjection mixes were prepared as follows: for *Ir8a*^{dsRED}, sgRNA (25 ng/μl), Cas9 mRNA (500 ng/μl), and donor plasmid (500 ng/μl) and, for *Ir8a*^{attP}, sgRNA (25 ng/μl), Cas9 mRNA (500 ng/μl), and

ssODN (500 ng/μl) were diluted into nuclease-free H_2O. A total of 1,069 and 509 embryos were injected to target exon 2 and exon 3, respectively.

Embryos were hatched 3 days after injection and reared to the adult stage as previously described [42]. A total of 50 G_0 females were sexed during pupation, allowed to mate freely with wild-type Orlando males, and females were blood-fed to generate G_1 progeny. G_0 females were put into oviposition vials to collect G_1 eggs. Thereafter, G_1 eggs were hatched and pupae were screened for *Ir8a*^{dsRED} insertion allele using a fluorescent microscope. Fluorescent G_1 individuals were sexed and reared to adulthood. Fluorescent females were outcrossed with wild-type animals for 5 generations and homozygosed.

The dsRED fluorescent protein gene insertion was detected in the *Ir8a* locus by PCR. Mosquito genomic DNA was purified using DNeasy Blood & Tissue kits (Catalog #69504, QIAGEN). PCR amplification was done using the following primers *Ir8a*^{dsRED}ForLA3 and Ir8aexon4rev3 (Table S1).

To further confirm site specific integration of the pGT-Ir8a donor DNA into *Ir8a* exon 2 and sequence the integration site, a 3483 bp PCR product was amplified using Novagen KOD polymerase (Catalog #71086-5, EMD Millipore) with the forward primer (*Ir8a*^{dsRED}ForLA3) homologous to the first 20 bp of *Ir8a* exon 2, which is also contained in the left arm of the donor plasmid, and the reverse primer (Ir8aexon4rev3) in *Ir8a* exon 4 outside the boundary of the right arm of the donor plasmid. This PCR product was then purified using NucleoSpin Gel and PCR cleanup kit (Catalog #740609, Machery-Nagel Inc., Bethlehem, PA, USA), cloned using the NEB PCR cloning kit (Catalog #E1202S, New England Biolabs) and Sanger sequenced using the SimpleSeq premixed Kit (Eurofins Genomics) with the following primers: Ir8adsRedForLA3, Ir8adsRedForLA1, Ir8aexon4rev3, Ir8a_polyU_For, Ir8adsRED_poly_rev2, Ir8a_afterRA_rev, and, SV40For1 (Table S1). Sequencing showed directed insertion into *Ir8a* exon 2 with no aberrant insertions or deletions.

Ir8a^{attP} mutant lines were screened for *attP* insertion and detected by fluorescent size-based genotyping each generation. Pupae were sexed and allowed to eclose in same-sex cages. Virgin G_2 females were allowed to mate freely with introduced wild-type males 24 hours after eclosion. Mosquitoes were then outcrossed to wild-type in this manner for 5 generations. Single-pair crosses of G_5 siblings were set up and mosquitoes with the desired mutations were chosen for homozygosing. Females were blood-fed and placed in individual oviposition vials. After eggs were laid, females were sacrificed, and genomic DNA was extracted using the IBI Genomic DNA extraction kit (Catalog #IB47222, IBI Scientific, Peosta, IA, USA). A fluorescent amplicon was generated using Amplitaq Gold 360 PCR master mix (Catalog #4398881, Applied Biosystems, Foster City, CA, USA) for each female using the following primers: Ir8aExon3for1 and Ir8aExon3rev2 (Table S1). Samples were sent for capillary electrophoresis to the DNA Core Lab at Florida International University and were then genotyped using Peak Scanner software (v1.0, Applied Biosystems) to determine the fragment length. To confirm the single stranded donor DNA insertion in the *Ir8a*^{attP} allele, PCR products were amplified from mosquitoes that contained the *Ir8a*^{attP} allele and were PCR purified using QIAEX II Gel Extraction Kit (Catalog #20051, QIAGEN). After purification, the amplicons were ligated into the pCR2.1 TOPO TA vector (Catalog #K462040, Invitrogen, Carlsbad, CA, USA) and transformed with One Shot TOP10 chemically competent *E. coli* cells (Catalog #C607003, Invitrogen). Thereafter, colonies were picked and prepped using the QIAprep Spin Miniprep Kit (Catalog #27104, QIAGEN). The plasmid DNA was sequenced in the DNA Core facility lab at the Florida International University.

Mosquito tissue dissection and preparation

In order to determine where *Ir8a* is expressed in adult female mosquitoes, we dissected five different body parts including the whole body, head without antennae, antennae alone, head alone, and headless body from sugar-fed 7–10 days old wild-type *Ae. aegypti* of the Orlando strain. A total of 10 mosquitoes were dissected for each body part except for the antennae, where a total of 25 antennal pairs were used for the assay. In addition, we also dissected antennal tissues from *Ir8a*$^{dsRED/dsRED}$, *Ir8a*$^{attP/dsRED}$, *Ir8a*^{dsRED}/+, *Ir8a*^{attP}/+, and wild-type *Ae. aegypti* Orlando strain to determine if *Ir8a* mRNA expression was altered by the mutations we made. For this assay, a total of 10 mosquito heads were used for each genotype. Using a pair of forceps, samples were dissected under cold anesthesia into RNAlater stabilization solution (Catalog #AM7020, Invitrogen) or into a dry ice/ethanol bath. For each genotype or tissue type. at least three biological replicates were used.

Ir8a mRNA extraction and treatment

Mosquito tissues were suspended in a 1 mL solution containing 4 M guanidine thiocyanate (CAS: 593-84-0), 0.5% Sarkosyl (CAS: 137-16-6), Chloroform (CAS 67-66-3), and 0.1 M 2-mercapthoethanol (CAS: 60-24-2). Thereafter, tissue samples were manually homogenized using RNase-free disposable pellet pestles (Catalog #12-141-364, Thermo Fisher Scientific). Phenol-chloroform phase separation was performed to separate the supernatant. This phase extraction process was repeated twice for the supernatant. RNA extraction was performed using the RNAid Kit supplied by MPBio (catalog #111007200). Beads were washed twice using RNA Wash concentrate before eluting in 20μl DEPC-treated water. Sample concentration and quality were determined using NanoDrop 2000c (Thermo Fisher Scientific).

cDNA synthesis and qPCR

The RNA extracted was treated with Turbo DNA-free kit (Catalog #AM1907, Invitrogen) to remove any DNA contamination. RNA was diluted to 50 ng/ul for each sample. cDNA library was created with reverse transcriptase using the SuperScript II RT reagent kit (Catalog # 18080-051, Invitrogen) and primed using oligo dT. Each reaction comprises 200ng RNA to make up a final volume of 20μl. After cDNA synthesis, samples were treated with RNase cocktail enzyme mix (Catalog #AM2286, Thermo Fisher Scientific). cDNA samples

were amplified using Amplitaq Gold 360 master mix (Catalog #4398901, Fisher Scientific) and primed by ribosomal protein L32 gene. Genomic contamination and PCR amplification was assessed by running the sample on an agarose gel electrophoresis.

Ae. aegypti Ir8a mRNA expression was quantified using RT-qPCR (Catalog #4345241, Thermo Fisher Scientific). Quantitative PCR was performed using TaqMan gene expression assay. The reaction consists of two sequence-specific PCR primers with a custom TaqMan probe (Catalog #4331348, Thermo Fisher Scientific) in 2X universal master mix. The TaqMan assay was performed with three technical replicates for each given biological replicate. The real-time PCR was performed using the TaqMan universal PCR master mix (Catalog #4324018, Thermo Fisher Scientific). The forward primer sequence (ATCAGTCCGATCGCTATGACAAG) and the reverse primer sequence (GGTTGTCAATACCTTTCGGCTTAC) were used as control primers (Table S1). Raw data was analyzed using SDS v1.5.1 software with the detection threshold set at 0.2. Outliers with Ct values greater by 0.5 from the nearest technical replicate were discarded. The ribosomal protein L32 gene was used as endogenous control to normalize between cDNA samples. Relative fold change was calculated as previously described [54].

Locomotor activity assay

Mosquito activity was monitored using Locomotor Activity Monitors (LAM 25; Trikinetics Inc., Waltham, MA, USA). Sugar-fed 5 to 7-day old female mosquitoes were singly aspirated into glass tubes (25 mm diameter, 125 mm long) directly from the cage without cold anesthesia. The glass tubes were sealed at both ends with cotton plugs. One of the cotton plugs was soaked in water and the other end was left dry. This was done in order to generate more activity in the tube. We hypothesized that mosquitoes would hygrotax to the wet end. The set up was maintained at 25-28°C and 75% relative humidity under a 14:10 light-dark cycle (lights on at 8 am). The movements of the mosquitoes triggered an infrared beam break. This was set to record at every second and tabulated into 1min bins. Bins with more than 60 beam breaks and trials that exceed 2000 beam breaks per day were excluded from the analysis. Activity count was recorded for 24 hours on the fourth full day of fasting.

CAFE assay

The capillary feeder (CAFE) assay was adapted for mosquitoes with slight modifications from the feeding study carried out on fruit flies [45, 46]. Female mosquitoes aged 5 to 7 days were starved from sugar for 24 hours but had unlimited access to water. After fasting, five mosquitoes were transferred into each polystyrene vial (95mm long, 27mm wide) and sealed with a cotton plug. Thereafter, two calibrated 5 μl capillary tubes (catalog #1904637, Blaubrand Intramark) were introduced into the vial by pushing it through the cotton. The capillary tubes were filled with 10% sucrose to the 5 μl mark. The assay lasted for 18 hours and feeding was estimated by recording the change in the sucrose volume. Control vials without mosquitoes were also set up to correct for water loss due to evaporation.

Fasting resistance assay

This assay was carried out accordingly as previously described [21]. A total of sixty male and sixty female mosquitoes from each of the five genotypes ($Ir8a^{dsRED/dsRED}$, $Ir8a^{attP/attP}$, $Ir8a^{dsRED}$/+, $Ir8a^{ttP}$/+ and wild-type) were tested for fasting resistance. Prior to the experiment, mosquitoes were fed on 10% sugar. Thereafter, each mosquito was aspirated into a fly vial (25 mm diameter, 95 mm long) containing 1 cotton ball soaked in 10 mL of distilled water and plugged with a cellulose acetate fly vial plug (Catalog # 49-101, Genesee Scientific, San Diego, CA, USA). In order to control for positional effects, vials were randomized for genotype and sex in the racks. Experiments took place in the behavior room at 25-28°C, 75% relative humidity under a 14:10 light-dark cycle (lights on at 8 am). To quantify fasting resistance, visual examination of the vials was carried out each day to observe for any movement. If no movement was noticed, the vial was tapped twice and visually inspected again. If the mosquito failed to move, it was scored as dead.

Electrophysiological studies

Electroantennogram (EAG) recordings were made using Ag-AgCl electrodes and glass capillaries filled with Ringer solution (8.0 g L^{-1} NaCl 0.4 g L^{-1} $CaCl_2$) connected to silver wire, which closed the electric circuit. Non-blood fed female mosquitoes (*Ae. aegypti*) were recorded at 3-4 days post-eclosion between 8am and 4pm. Mosquitoes were chilled for one minute before their bodies were secured between sticky tape and wax. The glass capillary connected to the indifferent electrode was placed within the eye of the mosquito, and the glass capillary connected to the recording electrode was connected to the tip of the antennae. The signals were passed through a high impedance amplifier (IDAC-4, Syntech 2004, Hilversum, Netherlands) and analyzed using a customized software package (Syntech EAG-Pro 4.6). Ten microliter aliquots of each chemical compound at a concentration of 1x 10^{-3} mg/mL were added onto a pre-cut filter paper (Whatman No. 1, 20 mm), which was inserted into sterilized Pasteur pipette. The stimuli were delivered via an air stream at a flow rate of 1 $L.min^{-1}$ with a puff (2 s duration) at 30 s intervals. Solvent control (Hexane) was tested at the beginning and end of each repetition. Each treatment contained 5 replicates.

The odor volatiles tested in the EAG experiment include: Geranylacetone (C.A.S. 689-67-8), 6-methyl-5-hepten-2-one (Sulcatone, C.A.S. 110-93-0), Linalool (C.A.S. 78-70-6), Dodecanal (C.A.S. 112-54-9), Lactic acid (C.A.S. 79-33-4) and were obtained from Sigma-Aldrich. Octanoic acid (C.A.S.124-07-2), Heptanoic acid (C.A.S. 111-14-8) and Butyric acid (C.A.S. 107-92-6) were supplied by ICN. Octanal (C.A.S. 124-13-0) and Nonanal (C.A.S. 124-19-6) were obtained from Chemicon:Acros. Limonene (C.A.S. 5989-27-5) and Nonanoic acid (C.A.S. 112-05-0) were supplied by Fluka. 2-ethyl hexanol (C.A.S. 104-76-7) was obtained from Lancaster; while 1-octen-3-ol (C.A.S. 3391-86-4) was supplied by Janssen Chimica.

Membrane-feeding assay

This assay was carried out as previously described with slight modifications [22]. A total of four 14 mm diameter glass-jacketed membrane feeders (#CG-1835-70, Chemglass) were connected in series using silicone tubing to a digital water bath (VWR international). The membrane feeder was prepared by stretching a thin layer of Parafilm M laboratory film (Catalog #PM996, Bemis) over the feeders. Thereafter, a total of 1000μl of defibrinated whole sheep blood without any added ATP (Hemostat Laboratories) was transferred into each feeder. A dimension of 10 cm by 10 cm squares of nylon sleeves (Duane Reade), previously worn for 12 hours by a human subject, were perforated and stretched over the Parafilm and tied around the feeder. For each trial, 4 cups of mosquitoes (n = 18-20) were set into their feeding positions in a room with regulated temperature (25°C) and relative humidity (75%). The assay was supplemented with CO_2 diffusion pads (8.0 cm by 11.5 cm; Tritech Research), placed at the edge of the cup, and set to release at a rate of 2500-2700ppm measured by a carbon dioxide monitor (Catalog # CO_2-100, Amprobe, Everett, WA). The blood in the membrane feeder was heated to 37°C to mimic human body temperature. For assays without heated blood, the temperature was maintained at room temperature (26°C). Feeding positions were alternated to control for position effects on the genotypes tested. The assay had a duration of 15 min. Blood fed mosquitoes were visually scored and any mosquitoes that appeared not to have blood fed were squashed between paper towels. If blood was found on the paper after squashing, the animal was scored as blood fed.

Uniport olfactometer assay

A custom-built uniport olfactometer constructed by the Engineering Department at Florida International University was built to assess female mosquito attraction to human host stimuli. The uniport olfactometer is made of a large plexiglass tube (75cm long and 13cm wide) attached to a small cylindrical trap (13cm long and diameter is 5cm wide) which houses the mosquitoes before the experiment. The other end of the plexiglass tube is a hollow box (length is 25cm, breadth is 20cm and diameter is 13cm) connected to the stimulus chamber. Carbon-filtered, humidified air and CO_2 are able to mix with the odorants in the stimulus chamber to attract mosquitoes that have been released from the trap. The CO_2 release rate in the stimulus chamber was measured by an acrylic flowmeter Model VFA-4-SSV (Dwyer Instruments Inc., IN, USA) set at 3 SCFH. The final concentration for CO_2 in the assay was maintained at 2500-2700ppm by a carbon dioxide monitor (Catalog # CO_2-100, Amprobe). Whereas, air flow rate was set at 21 standard cubic feet per hour by an air flowmeter (King Instruments CA, USA). The sealed design of the uniport, air filtration, and the positive pressure caused by the airflow in the apparatus isolated the assay from potential odors in the surrounding environment.

For each trial, approximately 20 female *Ae. aegypti* mosquitoes one-week post-eclosion were sorted under cold anesthesia (4 C) and placed in a small cylindrical trap. All females used in the assay had access to their mating partners but had not obtained a blood meal. Females were fasted with access to water for up to 24 hours prior to the assay. Pre-assay fasting and behavior experiments took place at 25°C and 70%–80% relative humidity. In our experiments, we tested multiple genotypes including wild-type, heterozygous *Ir8a* mutant ($Ir8a^{dsRED}$/+), homozygous *Ir8a* mutant ($Ir8a^{dsRED/dsRED}$), heteroallelic *Ir8a* mutant ($Ir8a^{attP/dsRED}$), homozygous *orco* mutant ($orco^{16/16}$), heteroallelic *orco* mutant ($orco^{5/16}$), homozygous *Ir8a* and *orco* double mutants ($Ir8a^{dsRED}$, $orco^{16}$), homozygous *Gr3* mutant ($Gr3^{cf.p/cf.p}$), heterozygous *Gr3* mutant ($Gr_3^{cf.p}$/+), and homozygous *Ir8a* and *Gr3* double mutants ($Ir8a^{dsRED}$, $Gr_3^{cf.p}$). Heteroallelic mutants were tested to control for background mutations that may have occurred independently in each line. Double mutants were tested to assess the epistatic interaction between the two genes.

To explore the behavior of these mosquito lines, starved mosquitoes were released from the small cylindrical trap and allowed to respond to the stimuli. After 8 min, the number of mosquitoes attracted by host cues were counted. The 8 min time point was determined empirically to produce consistently high responses. A blank trial with no odor stimulus was run to ascertain that the set-up was clean. Attraction greater than 20% indicates the presence of residual odor and the whole set up was cleaned up again with an odorless soap and allowed to air dry. Mosquitoes were scored as attracted if they were able to fly upwind through the tube into the attraction trap within the time frame. Mosquitoes that move out of the cylindrical trap within the assay period were scored as activated.

Human host uniport assay

A total of 15 human subjects were recruited for this assay. Each subject was tested twice to assess their attractiveness to mosquitoes in a uniport olfactometer as described above. All subjects were given informed consent before participating in the experiment and approved by the Florida International University Institutional Review Board. The volunteers were diverse in age (19 to 41 years), gender (Male = 7, Female = 8), and race (White [5], Hispanic [7], Asian [1], Black [2]). All of the human subjects were asked not to wear scented cosmetics, deodorants, or fragrances on the day of the assay. Any subject that did not follow our request was excluded from the study. Human subjects that adhered to this rule were asked to insert their forearm up to the elbow level into the stimulus chamber. The arm was inserted through a tight-fitted glove affixed to the olfactometer to prevent airflow between the assay and the room. None of the human volunteers were bitten by mosquitoes during the experiment.

Human odor perfumed nylon sleeves uniport assay

The toe sections of women's knee-high pantyhose (Hanes Brands Inc., NC, USA) were cut off with scissors. A single volunteer subject was used for this assay to control for differential attractiveness. The subject wore the nylon sleeves on the arm and stretched it toward the armpit. This was worn overnight for 12 hours while the subject did not shower or apply any scented products. The nylon sleeves were later retrieved from both arms and immediately tested on the library of mutants already generated, as well as the wild-type mosquitoes in the uniport olfactometer. New nylon sleeves perfumed with human odor were used for each day of testing without prior storage. Nylon sleeves that had not been previously worn were used as a negative control.

Lactic acid uniport assay

In order to test the response of wild-type and *Ir8a* mutant mosquitoes to lactic acid, we used the set up for the uniport olfactometer assay with slight modifications. Approximately 30 mosquitoes were used for each trial. A total of 4ml L-(+)- lactic acid solution (C.A.S. 79-33-4, catalog number 27714; 88%–92%, Sigma-Aldrich) was transferred by a pipette directly into the open lid of a polystyrene Petri dish (60mm diameter, 10mm height). The treatment was centrally placed in the stimulus port. For the control, the Petri dish was left blank. The number of mosquitoes attracted was recorded after 10 min. CO_2 concentration (2500ppm −2700ppm) was monitored by a carbon dioxide meter (Catalog # CO_2-100, Amprobe).

Measuring CO_2 abundance in the uniport olfactometer

Carbon dioxide monitor (Amprobe CO_2- 100, Everett, WA) was used to measure CO_2 release rate in a custom-built uniport olfactometer. In this experiment, air flow rate was maintained at 21 standard cubic feet per hour (SCFH) as measured by an airflow meter (King Instruments CA, USA). The final CO_2 concentration in the assay was measured by placing the CO_2 monitor at the end where the trapped mosquitoes were temporarily held before they were released to fly upwind. For the assay with air alone, carbon-filtered humidified air was released into the stimulus port. For the assay with supplemented CO_2, an acrylic flowmeter Model VFA-4-SSV (Dwyer Instruments Inc., IN, USA) set at 3 SCFH was used to control CO_2 release rate into the stimulus chamber of the uniport. For the assay with a human arm, the arm of the subject was inserted through a tight-fitted glove affixed to the olfactometer to prevent airflow between the assay and the room. The sealed design of the uniport and the positive pressure caused by the airflow in the apparatus isolate the assay from potential odors in the surrounding environment. The stimuli (airflow, supplemented CO_2 and skin-emanated CO_2) traveled from the stimulus port into the large plexiglass tube (75cm long and 13cm wide) and exited via the aperture where the mosquitoes were released. The CO_2 final concentration was measured via the aperture where the mosquitoes were released.

A total of ten trials were carried out to measure the CO_2 release rate from the olfactometer. The device was turned on and allowed to calibrate to ambient CO_2 room concentration. For each measurement, the device was placed in the aperture and measurements were recorded when the digital recording was stabilized. The device recording was stable when the beep sound was consistent. After taking the recording, the device was removed from the aperture and allowed to calibrate to ambient room condition. This process was repeated consistently for the ten trials. Carbon dioxide release rates were measured in three different conditions: humidified air, humidified air and CO_2, and humidified air supplemented with CO_2 and human arm. Data was analyzed using one-way ANOVA. Conditions marked with different letters were significantly different according to post hoc Tukey's HSD test.

QUANTIFICATION AND STATISTICAL ANALYSIS

Statistical analysis of our behavioral and quantitative PCR datasets was performed using the GraphPad Prism 7 software package (GraphPad Software, San Diego, CA, USA). Statistical analysis of our electrophysiological recordings (EAGs) were performed using GraphPad Prism 8 software package (GraphPad Software, San Diego, CA, USA). All details for statistical analysis including the statistical tests used, number of trials (n), number of animals, and how significance was determined can be found in the figure legends.

Current Biology, Volume *29*

Supplemental Information

Aedes aegypti Mosquitoes Detect Acidic Volatiles Found in Human Odor Using the IR8a Pathway

Joshua I. Raji, Nadia Melo, John S. Castillo, Sheyla Gonzalez, Valeria Saldana, Marcus C. Stensmyr, and Matthew DeGennaro

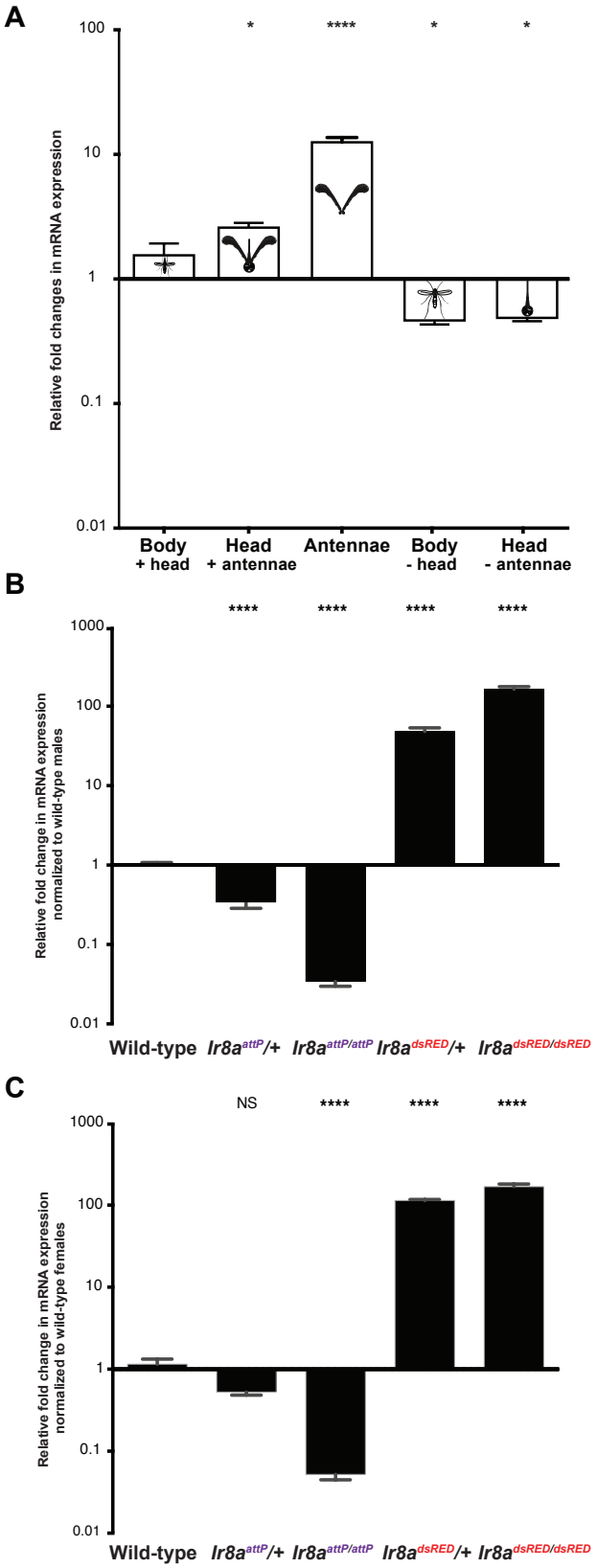

Figure S1: Quantification of *Ir8a* mRNA expression. Related to Figure 1.
(A) Quantitative RT-PCR analysis of *Ir8a* mRNA expression in wild-type female mosquito tissues. Bar plots represent the mean and standard error. Samples marked with asterisks are significantly different from an intact female by Mann-Whitney U test ($p < 0.0001$).(B) Relative fold change in mRNA expression normalized to wild-type males ($p < 0.0001$) and (C) females *Ae. aegypti* mosquitoes ($p < 0.0001$). Bar plots represent the mean and standard error. Data was analyzed by Mann-Whitney U test. Genotypes marked with asterisks are significantly different from wild-type controls.

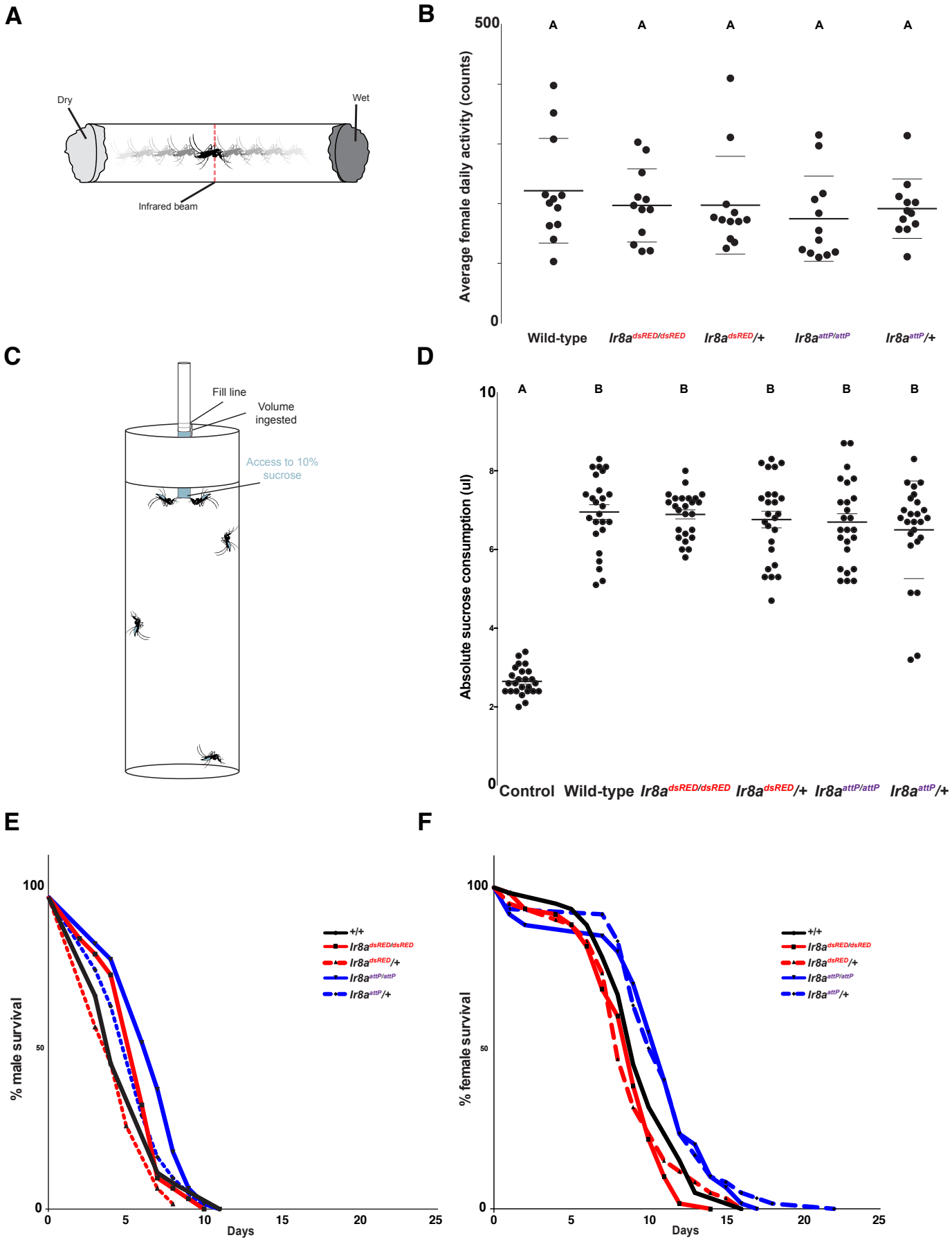
A
Dry
Wet
Infrared beam
B
Average female daily activity (counts)
500
0
A
A
A
A
A
Wild-type
Ir8a dsRED/dsRED
Ir8a dsRED/+
Ir8a attP/attP
Ir8a attP/+
C
Fill line
Volume ingested
Access to 10% sucrose
D
Absolute sucrose consumption (ul)
10
8
6
4
2
0
A
B
B
B
B
B
Control
Wild-type
Ir8a dsRED/dsRED
Ir8a dsRED/+
Ir8a attP/attP
Ir8a attP/+
E
% male survival
100
50
0
0
5
10
15
20
25
Days
+/+
Ir8a dsRED/dsRED
Ir8a dsRED/+
Ir8a attP/attP
Ir8a attP/+
F
% female survival
100
50
0
0
5
10
15
20
25
Days
+/+
Ir8a dsRED/dsRED
Ir8a dsRED/+
Ir8a attP/attP
Ir8a attP/+

Figure S2. Assessing locomotor activity, survival, and sugar-feeding behavior in *Ir8a* mutants. Related to Figure 1.

(A) Diagram of beam break assay to monitor mosquito locomotor activity. (B) Average daily locomotor activity of *Ir8a* mutants after 4 days of fasting measured by the number of infrared beam breaks (counts). On the dot plot, long lines represent the mean and short lines represent standard error. There were no statistical differences among genotypes ($p = 0.6224$, n = 12-13). (C) Diagram of Capillary Feeder (CAFÉ) assay to quantify feeding behavior in mosquitoes. (D) Cumulative sucrose consumption after 18 hours of sugar feeding ($p = 0.9411$, n=25). On the dot plot, long lines represent the mean and short lines represent standard error. Data was analyzed by one-way ANOVA, and genotypes marked with the same letters are not significantly different by post hoc Tukey's HSD test. (E) Percent survival of 300 females under sugar starvation (F) Survival of 300 males under sugar starvation. Data was analyzed using log rank test and Geahand-Wilcoxon test followed by pairwise log rank comparisons with Bonferroni correction (corrected significance threshold; $p < 0.001$). Using this test, $Ir8a^{attP/attP}$ males lived significantly longer than wild-type and $Ir8a^{dsRED/+}$. Whereas, $Ir8a^{attP/attP}$ female mosquitoes lived significantly longer than wild-type, $Ir8a^{dsRED/+}$, and $Ir8a^{dsRED/dsRED}$ mosquitoes. There was no difference for any other pair of curves.

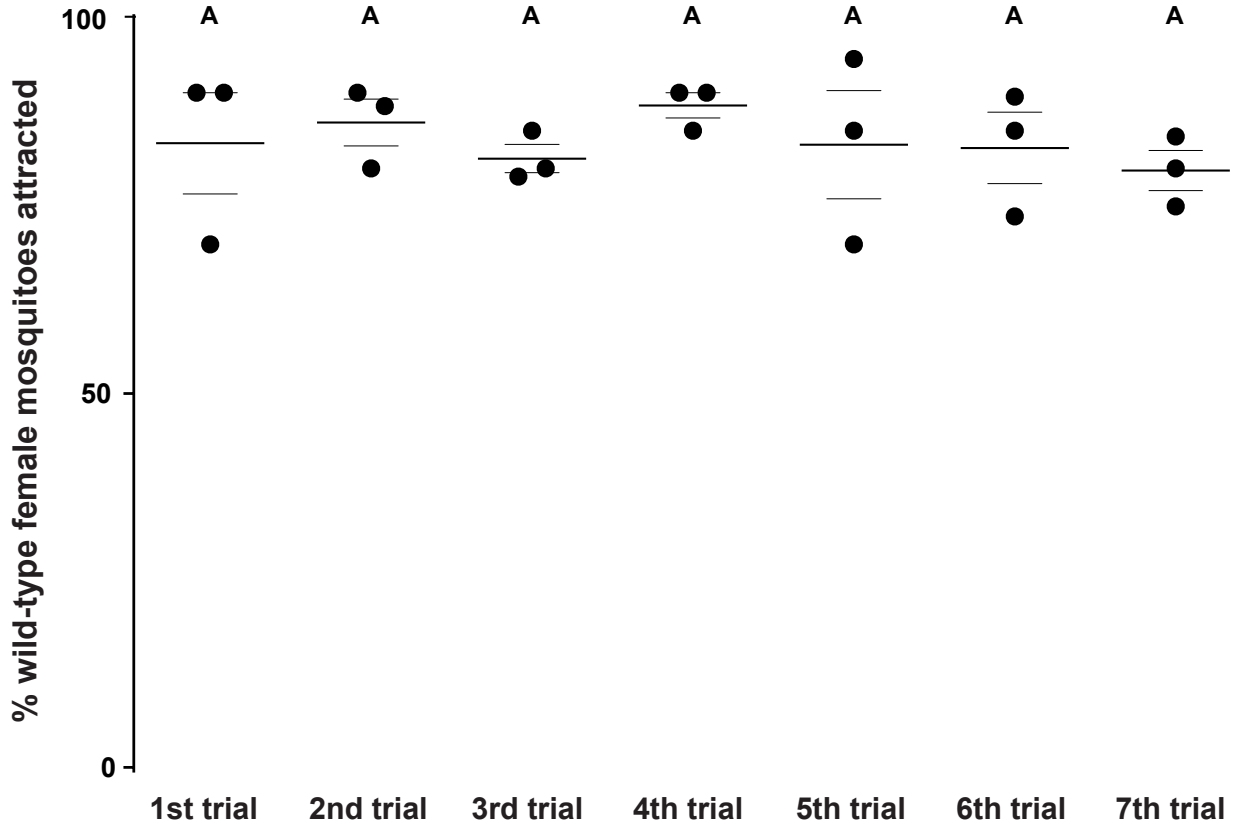

Figure S3: Time course experiment showing mosquito attraction to human-scented nylon sleeves. Related to Figure 4.

Percent wild-type mosquitoes attracted to human odor trapped on nylon sleeves (one-way ANOVA, n=3). The dot plot represents the mean and standard error. Genotypes marked with the same letters are not significantly different ($p = 0.8576$) by post hoc Tukey's HSD test.

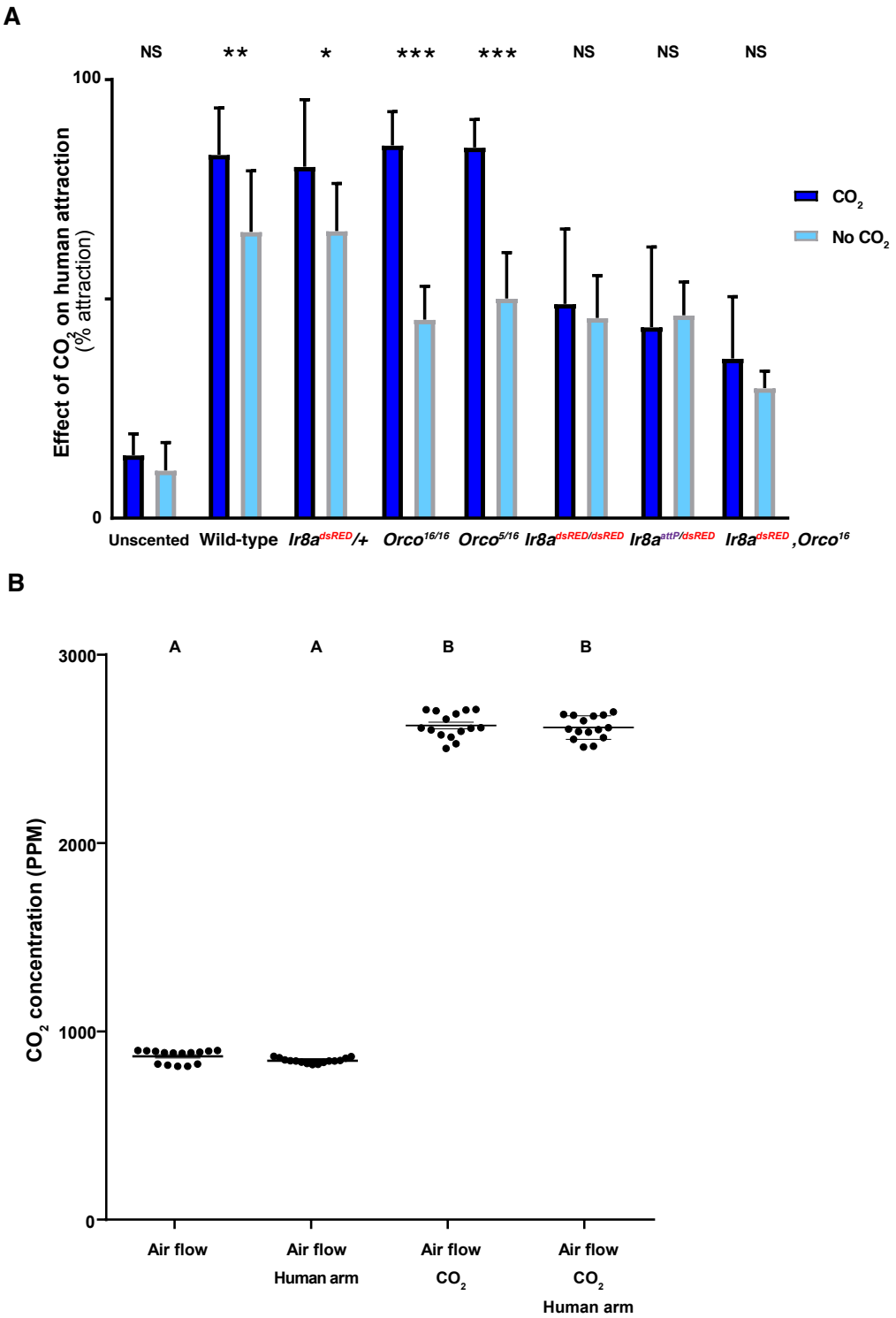

Figure S4: The attraction of *Ir8a* mutants to human odor is not modulated by the presence of CO_2. Related to Figure 4 & 5.

(A) Comparison of female mosquitoes attracted to human odor scented nylon sleeve in the presence and absence of CO_2. The bar plot represents the mean and standard error. Data compared is from figures 4C and 4F and analyzed by Two-way ANOVA, grouped column statistics comparing genotypes. Genotypes marked with asterisks are significantly different ($p < 0.001$).

(B) Measurement of Carbon dioxide concentration in the uniport olfactometer at different conditions with amprobe-100. The presence of a human arm in the assay did not significantly increase the concentration of CO_2. The addition of CO_2 to the assay significantly increase the amount of CO_2 concentration detected. Data was analyzed by one-way ANOVA followed by Tukey's multiple comparison test ($p < 0.0001$, n = 15).

Primer name	Sequence
IR8aExon2CRISPRF	GAAATTAATACGACTCACTATA**GGGCGGACAAAATGGCGTAT**GTTTTAGAGCTAGAAATAGC
IR8aExon3CRISPRF	GAAATTAATACGACTCACTATA**GGACATCTGTCGACGATAAC**GTTTTAGAGCTAGAAATAGC
sgRNArev	AAAAGCACCGACTCGGTGCCACTTTTTCAAGTTGATAACGGACTAGCCTTATTTTAACTTGCTATTTCTAGCTCTAAAAC
infusionIR8LA_1	CCATGATTACGAATTCCGGGTGTTTGGTTCTCCAGATTTG
infusionIR8LA_2	ATGGCCATTCGAATTCATAGCATGCGATGTAAGTGCAGGTAC
infusion_IR8RA1	ATGTACAGAGCTCGAGCGGTATTCGACTACTACATTGTCTAC
infusion_IR8RA2	ACTAGTACTTCTCGAGAGTACCGCTTGGTCGGTTTGATCTTC
Ir8a^{dsRED}ForLA3	GTTGTTCATGAACGTGAACAACCGG
Ir8aexon4rev3	CGTTTCCTGTAGGCCCAAGGG
Ir8adsRedForLA1	GAACGTGAACAACCGGAAGTACCT
Ir8a_polyU_For	GCGGCCCAAGTAAGCAGTG
Ir8adsRED_poly_rev2	CAGCAAGTGACGTCAACCCTTC
Ir8a_afterRA_rev	AACCTCGGTAGTTCCAACGCG
SV40For1	CTGCATTCTAGTTGTGGTTTGTCC
Ir8aExon3for1	6-FAM fluorescent modification- CGGATTCTCGGTTCTGGATG
Ir8aExon3rev2	CTCGGTAGTTCCAAGGCGAAAGTA
TaqMan Universal forward primer	ATCAGTCCGATCGCTATGACAAG
TaqMan Universal reverse primer	GGTTGTCAATACCTTTCGGCTTAC

Table S1: Table for oligonucleotides. Related to STAR methods. Table listing the primers and their corresponding oligonucleotide sequences used in the study. Nucleotide sequence in bold letters indicate the CRISPR target sequence.

Individual ID	Age	Race/Ethnicity	Sex
Subject 1	28	Black/African	M
Subject 2	22	Black	M
Subject 3	22	White/Hispanic	F
Subject 4	28	White	M
Subject 5	23	Hispanic	M
Subject 6	22	White/Hispanic	F
Subject 7	26	Hispanic	F
Subject 8	25	White	M
Subject 9	21	Hispanic	F
Subject 10	21	White	F
Subject 11	41	White/Hispanic	M
Subject 12	20	Asian	F
Subject 13	24	Hispanic	M
Subject 14	19	White	F
Subject 15	21	White	F
*Subject 16	24	White/Hispanic	M
*Subject 17	22	White/Hispanic	M
*Subject 18	41	White	M

Table S2: Human subject details for behavioral assays. Related to Figure 3, 4 & 5. Table showing the profile of the subjects used in the uniport olfactometer assay. Attraction to subject number 1 to 15 is shown in figure 4B. Subject number 1 was used exclusively to attract mosquitoes in host-seeking assays besides the uniport experiment represented in figure 4B. Subject 1 was used to control for individual differences that humans subjects present to mosquitoes. Asterisks indicate excluded subject. Subject number 16 to 18 were excluded from the experimental because they withdrew from the experiment or less than 20% of mosquitoes were attracted to them.